Non-Intrusive Load Modeling Using Newton-Phaselet Frames

by

Petrus Pijnenburg

Bachelor of Science in Engineering, Fontys, Eindhoven, 2013

A THESIS SUBMITTED IN PARTIAL FULFILLMENT OF THE REQUIREMENTS FOR THE DEGREE OF

Masters of Science in Engineering

In the Graduate Academic Unit of the Electrical and Computer Engineering

Supervisor:	Saleh, PhD, Electrical and Computer Engineering
Examining Board:	Kenneth B. Kent, PhD, Computer Science
	Eduardo Castillo-Guerra, PhD,
	Electrical and Computer Engineering

This thesis is accepted

Dean of Graduate Studies

THE UNIVERSITY OF NEW BRUNSWICK

April, 2015

©Petrus Pijnenburg, 2015

Abstract

Power system companies, including Canadian ones, have been making remarkable efforts towards implementing smart grid functions within their service domains. These efforts are spearheaded by establishing demand response programs for residential and small commercial loads (RSCLs). Demand response programs face a major challenge in their capacities to offer effective and economic options for customers in RSCLs, and thus fail to attract wide customer participation. The major challenge facing demand response programs is the lack of accurate models for energy demands and patterns of consumption in RSCLs. Available models of RSCLs are based on statistical methods, which require collecting significant amounts of data for energy demands of RSCLs over different hours each season. Statistical methods generally produce approximate models that may not accurately represent energy demands and patterns of consumption in RSCLs over different seasons. Furthermore, data collection from RSCLs can raise the costs of implementing smart grid functions, as extra instrumentation is required to monitor and record energy consumption of RSCLs.

The main objective of this research is to develop new models for RSCLs using numerical methods and orthogonal multi-frames. The proposed modeling method uses one value of the active power P to calculate one value of the apparent power $|\bar{S}|$, while it employs six phaselet frames to calculate a value of the angle θ (the phase of $\bar{S}$). Calculated $|\bar{S}|$ and θ are used to calculate a value of the active power Pc, which is compared to P in order to adjust $|\bar{S}|$ for the next Newton iteration. Calculated values of $Pc, |\bar{S}|$, and θ at each iteration are employed to determine a value of the reactive power Q at the same iteration.

Determined values for $Pc, |\bar{S}|, \theta$, and Q, for each value of P, are employed to complete

the constant impedance (Z), constant current (I) and constant power (P) modeling, commonly called the ZIP model, for RSCLs. In these loads, changes in the voltage, due to ON-OFF switching, are assumed negligible, where constant power and constant current loads become of a similar class in the ZIP model. The complete ZIP model has standardized parameters for the power consumption in each appliance, and thus the ON-OFF status of each appliance can be determined using its standardized parameter. This approach is implemented as an algorithm, and realized for performance evaluation using different sets of collected power measurements. Performance results show simple implementation, accurate determination of ON-OFF status, and a low memory requirement.

Acknowledgements

I would like to thank my supervisor, Dr. S. Saleh for his guidance and help with any concerns and problems I had along the way. His knowledge helped me increase my own and become more aware of the world of phaselets.

I would also like to thank my wife, Romy, for supporting and helping me every step of the way towards completion of my degree.

Lastly, I would like to thank my family and friends for their support through this entire venture.

Contents

Abstract ii

Acknowledgements iv

Contents v

List of Tables viii

List of Figures ix

1 Introduction 1

1.1 General 1

1.2 Overview of Demand Response 3

1.3 Motivation 4

1.4 Literature Review 5

1.5 Objectives 12

1.6 Thesis Outlines 13

2 ZIP Model for Residential Loads 14

2.1 General 14

2.2 Constructing the ZIP Model 15

2.2.1 Constant Impedance Loads 16

2.2.2 Constant Power Loads 18
2.3 Determining Power Changes Using the ZIP Model 20
2.4 Summary 22

3 Phaselet Analysis **23**
3.1 General 23
3.2 Multi-Resolution Analysis (MRA) 24
3.3 Phaselet Basis Functions and Frames 26
3.4 Realizing Phaselet Frames 28
3.5 Summary 32

4 Performance of Newton-Phaselet Method **34**
4.1 General 34
4.2 Developing an Algorithm for the Newton Phaselet Method 35
4.3 Performance Results 39
4.3.1 First Data Set 41
4.3.2 Second Data Set 44
4.3.3 Third Data Set 44
4.4 Summary 52

5 Conclusions and Future Work **53**
5.1 Summary 53
5.2 Conclusions 54
5.3 Contributions 55
5.4 Future Work 56

Bibliography **57**

Appendix **62**

A Definitions of Power Components in IEEE 1459-2000 Standard **62**

B Tight Frames **64**

Curriculum Vitae

List of Tables

4.1 Standardized values for K_{pF} and K_{qF} 40

4.2 Performance criteria for individual loads 48

4.3 Performance criteria of all data sets 51

4.4 Performance comparison of the Newton phaselet, ANN, and MC methods: 51

List of Figures

1.1 A schematic block diagram depicting a generic realization of the demand response program for residential units. P_k denotes the power meter reading of the k^{th} residential unit, while CN_k denotes the control action initiated for the k^{th} residential unit. 4

3.1 The scaling function of the *bior1.3*: (a) the scaling function $\phi(t)$ and (b) the magnitude spectrum $|\hat{\phi}(\omega)|$ 30

3.2 The low pass FIR filters associated with generated phaselet basis functions: (a) the magnitude spectrum of each $G_{pm}(\omega),\ m = 1, \ldots, 6$ and (b) the phase for each $G_{pm}(\omega)$. 31

3.3 The high pass FIR filters associated with generated phaselet basis functions: (a) the magnitude spectrum of each $H_{pm}(\omega),\ m = 1, \ldots, 6$ and (b) the phase for each $H_{pm}(\omega)$. 32

4.1 Flowchart for ZIP modeling using phaselet frames. Table 4.1 provides values of K_{pF} and K_{qF} for different household appliances. 39

4.2 Performance results from the first data set: (a) measured power and calculated power in per unit, (b) calculated apparent power $|\bar{S}|$ in per unit, (c) calculated angle θ in degrees, and (d) calculated reactive power Q in per unit. 42

4.3 Performance results from the first data set: (a) water heater ON-OFF status, (b) fridge ON-OFF status, (c) stove ON-OFF status, and (d) heater ON-OFF status. 43
4.4 Performance results from the first data set: (a) K_{pF}, (b) water heater ON-OFF status, (c) actual water heater readings, (d) K_{pF}, (e) fridge ON-OFF status, and (f) actual fridge readings. 45
4.5 Performance results from the second data set: (a) measured power and calculated power in per unit, (b) calculated apparent power $|\bar{S}|$ in per unit, (c) calculated angle θ in degrees, and (d) calculated reactive power Q in per unit. 46
4.6 Performance results from the second data set: (a) water heater ON-OFF status, (b) fridge ON-OFF status, (c) stove ON-OFF status, and (d) heater ON-OFF status. 47
4.7 Performance results from the third data set: (a) measured power and calculated power in per unit, (b) calculated apparent power $|\bar{S}|$ in per unit, (c) calculated angle θ in degrees, and (d) calculated reactive power Q in per unit. 49
4.8 Performance results from the second data set: (a) water heater ON-OFF status, (b) fridge ON-OFF status, (c) stove ON-OFF status, and (d) heater ON-OFF status. 50

Chapter 1

Introduction

1.1 General

During the past few years, power system operation and control have made remarkable progress towards implementing smart grid functions. These progresses, in conjunction with a growing public interest in energy saving, have triggered significant demands for monitoring and controlling the energy consumed by residential and small commercial loads (RSCLs). In response to these demands, several utilities have started to [1–3]:

i) Upgrade energy meters to smart meters;

ii) Construct two-way communication links with RSCLs;

iii) Establish utility-demand response programs;

iv) Increase levels of integrating renewable energy sources;

v) Implement energy saving initiatives that will attract wide sectors of costumers;

vi) Identify energy customers that can be subject to energy saving initiatives.

Recent energy market reports (see references [4] and [6]) have highlighted customers' concerns regarding the participation in demand response programs. Such concerns are raised due to the lack of information about identifying appliances with high energy consumptions, along with difficulties in obtaining patterns of energy consumption in controlled appliances. On one hand, this information can help customers in RSCLs take proper decisions on energy saving and benefit from time-of-use rates. On the other hand, this information can help utilities to accurately manage peak load conditions ([1–6] and[27–30]).

In order to answer customers' concerns and utilities' needs, several devices have been developed to collect data from individual appliances, and process this data to provide patterns for energy consumption, as well as methods to identify appliances. However, installing each of these devices requires a network of sensors as the power consumption of each appliance has to be collected. The complicated requirements of these devices, along with their high cost, have made them less attractive to customers in RSCLs. Another method has been developed based on the data collected using smart meters. This method is called the non-intrusive load monitoring (NILM), which has attracted customers and utilities due to its low cost and simple implementation [1, 2, 7, 8]. The development of the NILM method has facilitated obtaining information about patterns of energy consumption in RSCLs. This information is obtained through decomposing the time series of the active power $P(t)$ determined from readings of a smart meter. Such a decomposition is meant to provide a time series for the electric power consumed by each appliance, that is [1–3]:

$$P(t) = P_1(t) + P_2(t) + \ldots + P_d(t). \tag{1.1}$$

where P_i is the power consumed by appliance i.

Various approaches have been proposed to perform the decomposition of $P(t)$ into $P_1(t), P_2(t), \ldots, P_d(t)$ in order to implement NILM. These approaches include the statistical, pattern-recognition, and multiple-signature detection. The implementation of NILM using the previous approaches has shown good abilities to provide patterns of energy consumption in RSCLs [7–10]. However, the tendencies of existing NILM implementations to create pattern-based models, in order to identify appliances, imply collecting and analyzing several sets of data over various hours during different seasons. Such pattern-based models of appliances can be categorized as:

a - Single-state method, which provides models composed of identical ON/OFF edges with the average power consumption of the appliance in between.

b - Multi-state method, which provides models composed of different ON/OFF edges with signature-based characteristic for the power consumption of the appliance.

1.2 Overview of Demand Response

There are different ways to describe the functions performed by a demand response program. The diversity of loads subject to control, diversity of appliances subject to control, and diversity of initiating the control commands to loads and/or appliances within controlled loads, may create different realizations of the demand response programs. Fig. 1.1 shows a generic realization of the demand response program, where the power meter readings of residential units, as well as control action initiated for these loads, are communicated via wireless links. In general, power meter readings collected from residential units are used to model and update the status of specific appliances, which are commonly defined as target appliances. Such target appliances may include water heaters, heaters, and air conditioning systems. The

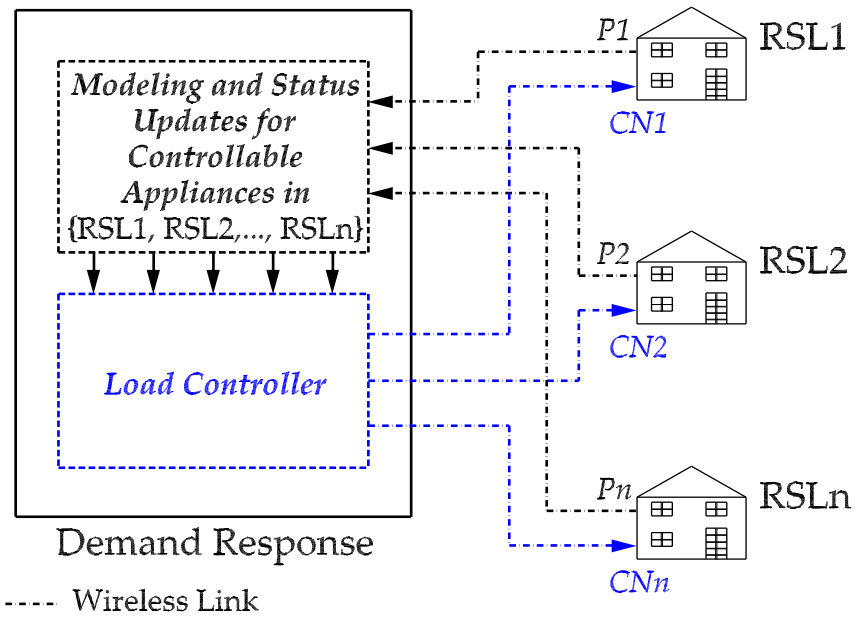

Figure 1.1: A schematic block diagram depicting a generic realization of the demand response program for residential units. P_k denotes the power meter reading of the k^{th} residential unit, while CN_k denotes the control action initiated for the k^{th} residential unit.

modeling and status updates of such appliances are required to initiate proper control actions ($\{CN\}_{k=1}^{k=n}$) by the load controller component of the demand response. There are several approaches for modeling the energy consumption of target appliances, such as statistical models, pattern recognition models, bottom- up models, etc. In this thesis, the ZIP model (described in Chapter 2) is to be used for modeling and status updates of target appliances.

1.3 Motivation

Several power companies have demonstrated growing interests in controlling power demands of RSCLs for purposes of establishing effective peak load management. These interests are based on the fact that power demands of RSCLs (mostly of

single phase (1ϕ) type) are among the major contributors to peak load conditions [1–5]. In general, peak load management of RSCLs can be achieved by [5–10]:

- direct load control (DLC);
- continuous two-way communication with consumers;
- tariff margins for certain consumer groups;
- demand response management.

The aforementioned approaches, for achieving peak load management, require accurate and instantaneous identification of power demands in RSCL, along with patterns of their energy consumptions. Such information is required for establishing direct load control, implementing demand response programs, and helping customers participate in energy saving initiatives[3–7].

1.4 Literature Review

The interests in implementing smart grid functions has motivated several research works that have been focused on realizing demand response programs in residential and small commercial loads (RSCLs), where peak-load management is the primary objective. These research works have identified that modeling the power demands and behaviors of RSCLs is the key element for realizing demand response programs, and achieve effective peak-load management. Several approaches have been proposed for modeling RSCLs in order to forecast their demands, and hence establish patterns for their energy consumptions.

The bottoms-up approach, presented in [9], has been among the early attempts to develop models for RSCLs. This modeling approach is based on a demand management system that is related to a bottom-up design. This design structure implies starting at the individual appliance level, and then work the way up to the total household level. These levels of load energy consumptions are defined as aggregation levels, which starts with level 1 that allows producing an individual household power demand profile. The second aggregation level is level 2 that provides an aggregation of the power demands for a group of different households. The bottom-up approach has been realized through an algorithm, called ARGOS, that collects data for individual households and determines the model for the data source, along with providing the energy consumption pattern for that household. The common sources for the data collected by ARGOS are the demographic/socioeconomic data, individual customer electricity usage habits, and engineering data operation of the relevant household appliances. The model offers an accurate prediction of individual loads if all appliances maintain a cyclic behavior over similar hours in similar seasons. The main limitations of the bottom-up approach is the need for a vast amount of historical data, which includes surveying of multiple household consumptions, obtaining demographic statistical data and probability of daily usage of individual devices etc. In addition, if one appliance has to be changed , then the ARGOS algorithm may not perform accurately as its purely based on previous data.

The gamma distribution algorithm has been proposed to forecast maximum demands for distribution networks [3]. This approach has offered an alternative method for the *after diversity maximum demand (ADMD)* method. The gamma distribution algorithm is based on analyzing the demand by collecting sample wattmeter readings from ordinary households. In this approach, the 3:00 PM temperature dependence of the daily energy use for a certain household on a particular day is combined

with the daily energy use values determined from a profile of collected wattmeter data, which collected with a sampling interval between 10 and 30 minutes from all households at hand [3]. The daily energy use for each household is generated by sampling the gamma distribution, where the random value is then corrected for the actual 3 pm temperature on the desired day in order to give a forecast of daily energy use. For each interval of the load profile, the simulated demands calculated by randomly sampling the second gamma distribution and scaling by the random energy use. This algorithm can be used for real time applications, where it may require few statistical data for completing its forecast. The major limitation of the gamma distribution approach includes the need for statistical data, which can increase the computational burdens and memory requirements. Moreover, the implementation of this modeling approach requires utilizing a stochastic process that demands continuous sampling for purposes of obtaining numerically correct values. Nonetheless, the introduction of the normalized terms in the gamma distribution approach has simplified its implementation, and has made it applicable for certain customized loads [3].

The peak load shifting approach, described in [7], has been developed for realizing new aggregation strategies, which are intended for overcoming the accuracy problems encountered due to the loss of load diversity. The loss of load diversity is generally caused by synchronous on/off equipment behaviors, peak shaving percentages, and peak-load shifting time of HVACs [7]. The aggregation strategies targeted by the load shifting approach are meant for improving the accuracy of load forecasting, as well as increasing the reliability of load direct controllers. The implementation of such aggregation strategies has raised concerns regarding their required computational capabilities, where intense stochastic processes are employed to obtain individual load projections and forecasts. Load projections and forecasts are accom-

plished by obtaining solutions for a third-order stochastic differential system (Monte Carlo), that is combined with an Euler-Maruyama discrete approximation method, or smoothing techniques realized by a numerical solution of the Fokker-Planck partial differential equations [7]. In these solutions, the main variables of interest are the probability density functions of the time-stamped indoor temperatures and power demands. Testing this modeling approach has revealed that the Fokker-Planck differential equations is faster and more accurate than the Monte Carlo equations. However, these differential equations require homogeneously grouped loads to ensure converging to a solution.

[8] proposes a stochastic approach for modeling loads. This approach is based on mapping different load types to residential neighborhoods. The implementation of this modeling approach has been accomplished by Monte Carlo numerical solvers, and the results have been compared with the calculated values at each time. The behavior in load is assumed to be always of a constant current nature, where it has a linear pattern with the average load traces. This assumption is justified by the fact that the majority of residential households have repetitive patterns of power demands and energy consumptions. The foundations for the stochastic modeling approach depend on picking some pre-recorded load traces in a residential load center, from which a certain consumer will be added as a new load trace. This addition of a new load trace is handled by the stochastic approach through calculating the percentile values. These calculations are repeated several times, after which the algorithm calculates the average value and standard deviation of the obtained percentile values. Finally, these calculations are repeated in order to determine the average and standard deviation for the sake of confirming its outcomes. The main challenge for this modeling approach is its computational demands, which are very high [8].

One of the modeling approaches has been developed based on tariff applications, as introduced in [2]. This approach has been proposed to assure users that they can have enough power to satisfy their demands, while maintaining their comfort levels. Such an insurance is made contingent with the ability of utilities to meet customer demands for energy at all times. The implementation of the tariff applications approach is based on disaggregating the load profile accurately into a sum of the load profiles for various appliances. The main goal of this disaggregation is to achieve a short term forecast of the residential energy consumption on an hourly basis. The desired load model is then computed for each hour of the day to create a pattern of energy consumption as a function of the apparent temperature. The tariff applications approach is generally implemented as Paatero-Lund(PL) model that uses two pieces of information from an appliance to model its energy consumptions. The first piece is the technological cycle which is a sequence of time segments tagged with levels of electric power consumption, where multiple cycles per appliances are ignored and are treated as a lumped load of several appliances with certain restrictions on simultaneous operations. The second piece needed is the probability of ON and OFF actions of any appliance at any time of the day. The obtained load model can be useful for many appliances for realizing demand side management. However, the statistical data required is hourly, which is relevant for a backup of the real time modeling [2].

The non-intrusive load monitoring (NILM) approach, presented in [1], is based on collecting data of electric energy consumption using reading of smart meters. The collected data is meant to create a history or a pattern of energy consumptions and operating statuses of major household appliances. The created pattern of energy consumption is intended to enable homeowners to make sound decisions on how to save energy and participate in demand response programs. The key idea for NILM

is to use the various signatures of the entire operating window of an appliance for accurate identification. The implementations of NILM have been achieved by utilizing two types of widows, that are [1]:

i) a window that contains one ON and one OFF event associated with one appliance;

ii) an overlapping window that contains one ON event associated with another appliance.

Both of the aforementioned windows contain five types of signatures, that are edge signatures, sequence signatures, trend signatures, time/duration signatures and phase signatures. In order to obtain a load model using NILM, the implementation algorithm has to be trained to detect and identify the events of individual appliances. The main goal for such identifications is to model appliances from only power meter readings, and dispense with additional instruments to measure power consumptions of each appliance. The major drawback for the NILM approach is mandates of extensive training, which requires collecting a significant amount of data from various appliances. The majority of training algorithms are designed using Artificial Neural Networks (ANN), which can be difficult to generalize without training for each appliance. In addition, in case of swapping any appliance, the entire algorithm needs to be retrained with new statistical data of the new appliance. There are several research works that are being conducted to facilitate and simplify the implementations of NILM for applications in real time load modeling for realizing smart grid functions.

The Artificial Neural Networks (ANN) have gained popularity in applications of load modeling. This approach offers reduced dependence on the nature of the modeled load, and facilitates creating accurate patterns for its energy consumptions. The em-

ployment of ANNs in modeling loads is proposed in [11], where rule-based structures is designed to determine a short-term forecasting of anomalous loads. The obtained models are generally based on four rules, each of which adds a different element to the algorithm. The only concern with these rules is that they may conflict with one another. In [12], another heuristic approach is proposed based on the Mamdani fuzzy model with multiple inputs and a single output to create a short-term load forecasts. The main difficulties with the heuristic approaches is due to their training data, which can be significant, and costly to collect. The other concern is their limited abilities for generalization without thorough training and settings.

Another methodology used in load modeling is the windowing function. This approach is based on the Fourier analysis, which compares a certain segment length (window) to a stream of data points. The window is represented by a filter bank that is usually composed of Finite Impulse Response (FIR) filters [15]. In the power system, this method would analyze a certain amount of power readings of an individual load at a time of a stream in order to calculate its change over time. the windowing technique will then throw out the historical data before moving onto the next segment of data. The length of segments vary depending on the application or type of load [16]. The problem with the window-based modeling approach is that a specific amount of historical data is required.

The major limitation of the aforementioned methods is their need for significant amounts of historical data that have to be collected over different hours in different seasons. Such a requirement implies using different instrumentation, data storage, and possibly communication means. Another challenge for the existing methods is due to the demands for processing power that is capable of handling the required computations, where large data is processed to obtain desired models. These challenges for modeling RSCLs are the driving motivation of this research work. The

main objective of this research work is to develop a modeling methodology for simple, economic, and historical-data free for RSCLs using only readings of a typical power meter in a household. The power data collected from power meters in RSCLs can be used on a one-reading basis for obtaining an instantaneous model of a RSCL. The instantaneous modeling is accomplished by determining the value of the reactive power for each value of the active power P. The determination of the reactive power in this research work is conducted using numerical iterations combined with phaselet frames. The main idea of such a method is to determine the magnitude of the apparent power $|\bar{S}|$ using Newton iterations, while the phase θ of the apparent power is determined using phaselet frames. Determined values of $|\bar{S}|$ and θ provide a value for the reactive power Q. The values of $P, \bar{S}, Q$, and θ can be employed for deriving the load model as a constant power load, constant impedance load, or constant current load at each collected value of P.

1.5 Objectives

The main objective of the research work in this thesis is to develop a new approach for modeling residential and small commercial loads (RSCLs) based on instantaneous readings obtained from household power meters. The Newton-phaselet approach is developed to calculate a value for the apparent power $\bar{S}$, the angle θ and reactive power Q for each value of the active power P. The values of $\bar{S}$, θ, Q and P are utilized to obtain the ZIP model for the RSCL of interest. Performance results of the Newton-phaselet approach demonstrate its accuracy, insensitivity to modeled loads, and simple implementation without needs for historical data.

1.6 Thesis Outlines

The thesis will be split into the following chapters:

i) Chapter 2 presents the general formulation of the ZIP model, and the simplifications that can be made for RSCLs. This chapter also provides the mathematical derivations to represent the changes in power demands of RSCLs using the simplified ZIP model.

ii) Chapter 3 briefly describes the processing of signals using sets of orthogonal basis functions, in particular using wavelet and phaselet basis functions. This chapter also presents the concept of processing signals using frames that are constructed by phaselet basis functions. Finally, Chapter 3 proposes the employment of phaselet frames to process signals for potential applications in power systems, particularly for calculating the power angle θ using values of the active power P in order to complete the ZIP model.

iii) Chapter 4 details the development of an algorithm to realize the Newton-phaselet method, and its implementation using MATLAB/SIMULINK software. The performance of the developed algorithm is also evaluated in this chapter for three sets of data collected from different residential units over different time intervals.

iv) Chapter 5 presents a summary of this thesis, along with the conclusions drawn from the performance results of the Newton-phaselet method for modeling and updating the ON-OFF status of appliances in residential units. Finally, this chapter identifies some avenues for future research works that can be based on the presented research work.

Chapter 2

ZIP Model for Residential Loads

2.1 General

The main objective of this research work is to develop a new modeling approach for residential and small commercial loads (RSCLs) using only instantaneous readings of a power meter in these loads. The foundations of the proposed modeling approach are based on the generic load classes, that are:

- Constant power loads;
- Constant current loads;
- Constant impedance loads.

These load classes are commonly called the *ZIP model*. The ZIP model is very common in modeling loads and power demands for power system analysis, planning, design, and transient analysis. The general ZIP model can be described in terms of

the active and reactive power demands of the modeled load as:

$$P = P_o \left(P_Z \left(\frac{V}{V_o} \right)^2 + P_I \left(\frac{V}{V_o} \right) + P_S \right) (1 + K_{pf} \Delta f) \tag{2.1}$$

$$Q = Q_o \left(Q_Z \left(\frac{V}{V_o} \right)^2 + Q_I \left(\frac{V}{V_o} \right) + Q_S \right) (1 + K_{qf} \Delta f) \tag{2.2}$$

where V is the voltage, V_o is the rated voltage of the modeled load, P_o and Q_o are the active and reactive powers ratings of the modeled load, P_Z and Q_Z are components in the active and reactive power demanded by the constant impedance part of the modeled load, P_I and Q_I are components in the active and reactive powers demanded by the constant current part of the modeled load, P_S and Q_S are components in the active and reactive powers demanded by the constant power part of the modeled load, k_{pf} and K_{qf} are parameters that represent the frequency sensitivity to variations in P and Q, respectively, and f is the frequency.

2.2 Constructing the ZIP Model

The ZIP model can be used for modeling RSCLs, where the instantaneous power demands (P and Q) can be composed of the demands of different appliances. In general, appliances in any RSCL can be mapped into constant impedance, constant current, and constant load classes. In order to employ the ZIP model in RSCLs, the following assumptions have to be made:

i- Switching ON or OFF an appliance does not significantly change the voltage V: $V \approx V_o$;

ii- Switching ON or OFF an appliance does not significantly change the frequency f: $\Delta f \approx 0$.

These assumptions can be concluded as $P_I \approx P_S$, and $Q_I \approx Q_S$, as $V \approx V_o$. The previous approximations and assumptions simplify equations (2.1) and (2.2), that is:

$$P = P_o\,(P_Z + 2P_S) \tag{2.3}$$

$$Q = Q_o\,(Q_Z + 2Q_S) \tag{2.4}$$

When an appliance is switched ON or OFF, the model of the RSCL will change, where such a switching action can be seen as changes in P and/or Q as:

$$P \pm \Delta P = P_o\,(P_Z \pm \Delta P_Z + 2P_S \pm \Delta P_S) \Longrightarrow \Delta P = P_o\,(\Delta P_Z + 2\Delta P_S) \tag{2.5}$$

$$Q \pm \Delta Q = Q_o\,(Q_Z \pm \Delta Q_Z + 2Q_S \pm \Delta Q_S) \Longrightarrow \Delta Q = Q_o\,(\Delta Q_Z + 2\Delta Q_S) \tag{2.6}$$

Equations (2.5) and (2.6) indicate that an instantaneous model of a RSCL can be derived from ΔP and/or ΔQ, if the individual changes $\Delta P_Z, \Delta P_S, \Delta Q_Z$, and ΔQ_S can be determined. ΔP_Z and ΔQ_Z are components of the constant impedance class while ΔP_S and ΔQ_S are representations of the changes in constant power and constant current components of the general ZIP model.

2.2.1 Constant Impedance Loads

These loads have fixed impedances, where the active and/or reactive power demands may change as a result of changes in the current drawn or the voltage applied to such loads. The active and reactive power demands for such loads can be stated as:

$$P_Z = \frac{V^2}{Z}\cos(\theta) \tag{2.7}$$

$$Q_Z = \frac{V^2}{Z}\sin(\theta) \tag{2.8}$$

The change in the active power demand of a constant impedance load can expressed in terms of its voltage, impedance, and power angle θ. It should be noted that in case of a RSCL, the voltage can be assumed constant, which simplify stating the changes in the active and/or reactive power demands for a constant impedance load as:

$$P_Z + \Delta P_Z = \frac{V^2}{Z}\cos(\theta + \Delta\theta) \tag{2.9}$$

Employing trigonometric identities, the above equation can be stated as:

$$P_Z + \Delta P_Z = \frac{V^2}{Z}\left(\cos(\theta)\cos(\Delta\theta) - \sin(\theta)\sin(\Delta\theta)\right) \tag{2.10}$$

For a small angle α, $\cos(\alpha) \approx 1$, and $\sin(\alpha) \approx \alpha$. Utilizing these approximations in the previous equation yields:

$$P_Z + \Delta P_Z = \frac{V^2}{Z}\left(\cos(\theta) - \Delta\theta\sin(\theta)\right) = \frac{V^2}{Z}\cos(\theta) - \frac{V^2}{Z}\Delta\theta\sin(\theta) \tag{2.11}$$

The above equation can be simplified as:

$$\Delta P_Z = -\frac{V^2}{Z}\Delta\theta\sin(\theta) \tag{2.12}$$

If the change in reactive power is to be considered (with the assumption of a constant voltage), it can be stated as:

$$Q_Z + \Delta Q_Z = \frac{V^2}{Z}\sin(\theta + \Delta\theta) \tag{2.13}$$

Employing trigonometric identities, the previous equation becomes:

$$Q_Z + \Delta Q_Z = \frac{V^2}{Z}\left(\sin(\theta)\cos(\Delta\theta) + \cos(\theta)\sin(\Delta\theta)\right) \tag{2.14}$$

The approximated values of sin(.) and cos(.) for a small angle can be used to simplify equation (2.37), that is:

$$Q_Z + \Delta Q_Z = \frac{V^2}{Z}\left(\sin(\theta) + \Delta\theta\cos(\theta)\right) = \frac{V^2}{Z}\sin(\theta) + \frac{V^2}{Z}\Delta\theta\cos(\theta) \tag{2.15}$$

The previous equation can be reduced to:

$$\Delta Q_Z = \frac{V^2}{Z}\Delta\theta\cos(\theta) \tag{2.16}$$

2.2.2 Constant Power Loads

These loads have a constant apparent power demand, where the active and reactive powers may change. However, the changes in the active and reactive powers will always yield constant apparent power.

$$|\bar{S}|^2 = P^2 + Q^2 \tag{2.17}$$

$$|\bar{S} + \Delta\bar{S}|^2 = (P + \Delta P)^2 + (Q + \Delta Q)^2 \tag{2.18}$$

$$|\bar{S}|^2 + 2\bar{S}\Delta\bar{S} + \left(\Delta\bar{S}\right)^2 = P^2 + 2P\Delta P + (\Delta P)^2 + Q^2 + 2Q\Delta Q + (\Delta Q)^2 \tag{2.19}$$

Assuming that square the change is very small as $\left(\Delta\bar{S}\right)^2 \approx (\Delta P)^2 \approx (\Delta Q)^2 \approx 0$, produces:

$$|\bar{S}|^2 + 2\bar{S}\Delta\bar{S} = P^2 + 2P\Delta P + Q^2 + 2Q\Delta Q \Longrightarrow \bar{S}\Delta\bar{S} = P\Delta P + Q\Delta Q \tag{2.20}$$

For a constant power load, the change in $\bar{S}$ will be zero as P and/or Q change, that is:

$$0 = P\Delta P + Q\Delta Q \Longrightarrow \Delta P = -\frac{Q}{P}\Delta Q \tag{2.21}$$

Substituting $Q = P\tan(\theta)$ in the above equation yields:

$$\Delta P = -\Delta Q \tan(\theta) \tag{2.22}$$

In order to express ΔQ in terms of ΔP, the relationship between P and Q is employed as:

$$Q = P\tan(\theta) \Longrightarrow Q + \Delta Q = (P + \Delta P)\tan(\theta + \Delta\theta) \tag{2.23}$$

Utilizing the trigonometric identity for the tan function as:

$$\tan(a + b) = \frac{\tan(a) + \tan(b)}{1 - \tan(a)\tan(b)} \tag{2.24}$$

Using the trigonometric identity, and the approximation that for a small angle α: $\tan(\alpha) \approx \alpha$, the equation for ΔQ can be expressed, with approximating $\Delta P\Delta\theta \approx 0$, as:

$$Q+\Delta Q = (P+\Delta P)\left(\frac{\tan(\theta) + \Delta\theta}{1 - \Delta\theta\tan(\theta)}\right) = \frac{P\tan(\theta)}{1 - \Delta\theta\tan(\theta)} + \frac{\Delta P\tan(\theta)}{1 - \Delta\theta\tan(\theta)} + \frac{P\Delta\theta}{1 - \Delta\theta\tan(\theta)} \tag{2.25}$$

Another approximation can be made since $\Delta\theta\tan(\theta)$ is very small, that is:

$$Q \approx \frac{P\tan(\theta)}{1 - \Delta\theta\tan(\theta)}$$

The previous approximations simplify the expression for ΔQ to:

$$\Delta Q = \frac{\Delta P \tan(\theta)}{1 - \Delta\theta \tan(\theta)} + \frac{P\Delta\theta}{1 - \Delta\theta \tan(\theta)} \tag{2.26}$$

Substituting equation (2.26) into equation (2.22) yields:

$$\Delta P = -\frac{\Delta P \tan^2(\theta)}{1 - \Delta\theta \tan(\theta)} - \frac{P\Delta\theta \tan(\theta)}{1 - \Delta\theta \tan(\theta)} \tag{2.27}$$

Simplifying equation (2.27) produces:

$$\Delta P = -\frac{P\Delta\theta \tan(\theta)}{1 - \Delta\theta \tan(\theta) + \tan^2(\theta)} \tag{2.28}$$

If the change in the reactive power for a constant power load is to be considered, then equation (2.22) can be used to express the change in Q as:

$$\Delta Q = \frac{\Delta P}{\tan(\theta)} \tag{2.29}$$

Substituting equation (2.27) into equation (2.29) provides the change in reactive power for a constant power load as:

$$\Delta Q = \frac{P\Delta\theta}{1 - \Delta\theta \tan(\theta) + \tan^2(\theta)} \tag{2.30}$$

2.3 Determining Power Changes Using the ZIP Model

The simple approach to determine values for $\Delta P_Z, \Delta P_S, \Delta Q_Z$, and ΔQ_S can be set through the general relationship between the apparent power, active power, and

reactive power, that is:

$$|\bar{S}|^2 = P^2 + Q^2 \Longrightarrow \left(|\bar{S}| + \Delta|\bar{S}|\right)^2 = (P + \Delta P)^2 + (Q + \Delta Q)^2 \tag{2.31}$$

Expanding the change in $|\bar{S}|$ (due to an ON or OFF switching action), produces:

$$|\bar{S}|^2 + 2|\bar{S}|\Delta|\bar{S}| + \left(\Delta|\bar{S}|\right)^2 = P^2 + 2P\Delta P + (\Delta P)^2 + Q^2 + 2Q\Delta Q + (\Delta Q)^2 \tag{2.32}$$

If the square changes are assumed very small, that is $\left(\Delta\bar{S}\right)^2 \approx (\Delta P)^2 \approx (\Delta Q)^2 \approx 0$, then:

$$|\bar{S}|^2 + 2|\bar{S}|\Delta|\bar{S}| = P^2 + 2P\Delta P + Q^2 + 2Q\Delta Q \Longrightarrow |\bar{S}|\Delta|\bar{S}| = P\Delta P + Q\Delta Q \tag{2.33}$$

The expression in equation (2.33) provides a general setting for the changes in the power due to any switching action. In order to identify the source of a switching action, i.e. a constant impedance or a constant power load, equation (2.33) has to be applied for both load classes. Appendix I provides detailed derivations for both load classes. These derivations provide the following changes in the power due to a switching action:

- *Constant power load*:

$$\Delta P_S = -\frac{P\Delta\theta\tan(\theta)}{1 - \Delta\theta\tan(\theta) + \tan^2(\theta)} \tag{2.34}$$

$$\Delta Q_S = \frac{P\Delta\theta}{1 - \Delta\theta\tan(\theta) + \tan^2(\theta)} \tag{2.35}$$

  where θ is the phase of the apparent power $\bar{S}$.

- *Constant impedance load*:

$$\Delta P_Z = -\frac{V^2}{Z}\Delta\theta\sin(\theta) \tag{2.36}$$

$$\Delta Q_Z = \frac{V^2}{Z}\Delta\theta\cos(\theta) \tag{2.37}$$

2.4 Summary

This chapter has presented an overview of the ZIP model for application in Residential and Small Commercial Loads (RSCL). The formulation of the ZIP model is based on decomposing the active and reactive power demands of any RSCL into three basic load classifications: constant impedance, constant current, and constant power. However, since voltage changes in RSCLs can be assumed negligible, the ZIP model for such loads can be reduced into constant impedance and constant power component.

The general formulation of the ZIP model requires both the active and reactive power demands of the modeled loads. Since typical power meters in RSCLs provide only reading for P (energy readings over fixed time interval), the determination of Q can be achieved by numerical iterative methods. Such a numerical method is proposed to be structured from Newton iterations and phaselet frames. The next chapter describes constructing phaselet frames for employment in completing the ZIP model for RSCLs.

Chapter 3

Phaselet Analysis

3.1 General

Orthogonal and orthonormal basis functions possess several capabilities, such as spanning dense and/or complete spaces, producing finite impulse response (FIR) filters, constructing frames etc. A space is a collection of basis functions that have to satisfy certain conditions, including linear independence and orthogonality. A set of D basis functions, $\{\beta_0(t), \beta_1(t), ..., \beta_{D-1}(t)\}$, can span a space V, that is:

$$V = \text{clos}_{L^2(\mathbb{R})} \langle \{\beta_d(t)\} \rangle . \tag{3.1}$$

where $L^2(\mathbb{R})$ is the space of square-integrable functions and $D \in \mathbb{R}$ or $D \in \mathbb{Z}$. Any signal or function $x(t) \in V$ can be decomposed using the set of basis functions $\{\beta_0(t), \beta_1(t), ..., \beta_{D-1}(t)\}$ as:

$$x(t) = \sum_{d=1}^{D-1} c_d \beta_d(t) \tag{3.2}$$

where c_d is a non-zero real number ($c_d \in \mathbb{R}$) and can be expressed as:

$$c_d = \left\langle x(t), \tilde{\beta}_d(t) \right\rangle \tag{3.3}$$

where $\tilde{\beta}_d(t)$ is the dual basis function of $\beta_d(t)$ and $\langle . \rangle$ is the inner product operation, which can be defined for any two functions $u(t)$ and $v(t)$ as:

$$\langle u(t), v(t) \rangle = \int_{-\infty}^{\infty} u(t).v^*(t)dt \tag{3.4}$$

where $v^*(t)$ is the complex conjugate of $v(t)$. It should be noted that for some basis functions, c_d can be a complex number.

One of the popular sets of basis functions with the capabilities of spanning successive dense and complete spaces are the wavelet basis functions. Spanned spaces by wavelet basis functions are generally used to construct multi-resolution analyses (MRAs). Wavelet based MRAs have demonstrated stable and converging features for a wide range of applications, including multi-stage expansion and successive approximations of signals, with unknown sources. The later feature is employed in this work to determine the apparent power (magnitude ($|\bar{S}|$) and phase (θ)) consumed by an unknown load.

3.2 Multi-Resolution Analysis (MRA)

The concept of successive approximations of a processed signal can be realized by sets of orthogonal basis functions. In each stage, a finite set of coefficients that represent the energy content of the processed signal is produced. The basis functions, used in constructing an MRA, are generated by integer shifts and dyadic (powers of 2) dilates of a real single function, which is known as the scaling function ($\phi(t)$) as

[17–19]:

$$\{\phi_{j,k}(t)\} := \left\{\phi\left(2^j t - k\right)\right\};\ k, j \in \mathbb{Z} \tag{3.5}$$

The basis functions ($\{\phi_{j,k}\}$) at scale j span a space V_j that provides one stage for approximating the processed signal. The spanned spaces by $\{\phi_{j,k}(t)\}$ can be formulated as [17–19]:

$$...V_{j-1} \subset V_j \subset V_{j+1} \subset V_{j+2}.... \tag{3.6}$$

The collection of nested spaces can be used to construct an MRA as [17–19]:

$$\text{MRA} = \bigcup_{j=0}^{\infty} V_j(\phi) \tag{3.7}$$

It can be shown that the MRA of a signal is one approach to approximate $x(t)$ through successive projections of $x(t)$ onto each space of the MRA, that is:

$$P_j(x(t)) = \sum_k \langle x, \phi_{j,k} \rangle \, \tilde{\phi}_{j,k} \tag{3.8}$$

The signal $x(t)$ can be recovered from its projections as:

$$x(t) = \lim_{j \to \infty} \left(\sum_j P_j(x(t)) \right). \tag{3.9}$$

In the case of processing a discrete signal $x_d[n]$, the successive approximations can be linked to digital filtering $x_d[n]$ using filters with dyadic pass and stop bands. The successive filtering of a discrete signal $x_d[n]$ can be viewed as approximating that signal in terms of its frequency components, which are extracted at each stage of approximation. Such successive filtering of $x_d[n]$ can be a setting for an MRA, constructed by digital half-band high pass and low pass FIR filters. The coefficients

of these FIR filters are obtained by solving the dilation equations, that are:

$$\phi(t) = \sqrt{2} \sum_{k} g[n]\phi(2t - k) \tag{3.10}$$

$$\psi(t) = \sqrt{2} \sum_{k} h[n]\phi(2t - k) \tag{3.11}$$

The processing of a signal as in equation (3.9) relates the generic MRA structure to infinite successive approximations. However, for purposes of realizing an MRA in practical applications, the number of resolution levels (stages of approximations) has to be finite, that is $j < \infty$. Such a requirement implies that the frequency contents of a processed signal can be extracted over a finite number of frequency sub-bands, and energy contents of that processed signal can be parametrized by a finite number of coefficients. The setting of $j < \infty$ and $k < \infty$ can cause an MRA to become shift-variant for processing some discrete signals ([20–22]). In order to maintain the shift-invariant feature of an MRA (with $j < \infty$ and $k < \infty$), each basis function, in a scale j, is modulated by a unit norm frame, which is composed of sine and cosine functions. This modulation causes the finite number of basis functions to construct an MRA with a shift-invariant feature ([20–22]). Such basis functions are defined as phaselet basis functions. The next section provides an overview of phaselet basis functions, along with some of their properties.

3.3 Phaselet Basis Functions and Frames

A frame is a generalized set of basis functions that can define a wavelet system $W \subset L^2(\mathbb{R})$ as [17–22]:

$$W\left(\{\psi_\ell\}_{\ell=1}^{r}\right) := \left\{2^{j/2}\psi_\ell\left(2^j t - k\right) : 1 \leq \ell \leq r; j, k \in \mathbb{Z}\right\}. \tag{3.12}$$

The system W is a tight wavelet frame in $L^2(\mathbb{R})$ if for any signal $x \in L^2(\mathbb{R})$:

$$\|x\| = \sum_{\ell=1}^{r} |\langle x, \psi_\ell \rangle|^2. \tag{3.13}$$

where $\langle . \rangle$ is the inner product and $\|.\|$ is the Euclidean norm. The notation of wavelet frames is generalized by defining lower and upper bounds ($A \in \mathbb{R}$ and $B \in \mathbb{R}$ with $0 < A \leq B < \infty$ (see Appendix II). Incorporating such bounds, the system W is a wavelet frame if it satisfies [17–20]:

$$A \|x\|^2 \leq \sum_{\ell=1}^{r} | \langle x, \psi_\ell \rangle |^2 \leq B \|x\|^2 . \tag{3.14}$$

It should be noted that for a tight wavelet frame $A = B = 1$. Another capability of wavelet functions is the generation of phaselet basis functions. Phaselet basis functions are one class of wavelet basis functions that offer supporting shift-invariant time-frequency transforms with reduced redundancy. A set of phaselet basis functions, $\{\alpha_m(t)\}_{m=0}^{M-1}$, with $m, M \in \mathbb{Z}$, can be generated by a real-valued scaling function $\phi_o(t)$. Each $\alpha_m(t)$ has a similar magnitude spectrum to that of $\phi_o(t)$. However, each $\alpha_m(t)$ has a unique phase τ_m. These features of phaselet basis functions can be stated as [17–22]:

$$\left|\hat{\alpha}_m\left(2^{-j}\Omega\right)\right| = \left|\hat{\phi}_o\left(2^{-j}\Omega\right)\right| e^{i\tau_m}. \tag{3.15}$$

where $\hat{\alpha}_m(\Omega)$ and $\hat{\phi}_o(\Omega)$ are the Fourier transforms of $\alpha_m(t)$ and $\phi_o(t)$, respectively, and i is the complex operator ($i = \sqrt{-1}$). The phases $\{\tau_m\}_{m=0}^{M-1}$ can be selected with a uniform distribution over $[-\pi, \pi]$ as :

$$\tau_m = -\frac{2\pi m}{M};\ \tau_m \in \mathbb{R},\ \text{and } m = 0, 1, 2, \ldots, M-1. \tag{3.16}$$

The phases defined in equation (3.16) have to meet the following condition [20–22]:

$$\sum_{m=0}^{M-1} e^{i\tau_m} = \sum_{m=0}^{M-1} e^{-i\frac{2\pi m}{M}} = 0 \text{ for } M \geq 2. \tag{3.17}$$

Among the advantages of phaselet basis functions is their ability to construct optimized frames, which have demonstrated promising applications in image and speech processing (see reference [20]). In this research work, the phaselet frames are to be used for a new application in power systems, in particular, for estimating the power consumption of unknown loads.

3.4 Realizing Phaselet Frames

Due to their ability to support time-frequency transforms, phaselet basis functions are associated with half-band digital low pass and high pass finite impulse response (FIR) filters. In general, a set of wavelet basis functions (including phaselet basis functions), $\left\{\psi_{(j,k)}\right\}$, $j, k \in \mathbb{Z}$, form a frame in $L^2(\mathbb{R})$, where any signal $x \in L^2(\mathbb{R})$ can be processed (decomposed and synthesized) as [17–22]:

$$x = \sum_{j\in\mathbb{Z}} \sum_{k\in\mathbb{Z}} \left\langle x, \psi_{(j,k)} \right\rangle \tilde{\psi}_{(j,k)}. \tag{3.18}$$

where $\psi_{(j,k)}(.) = 2^{j/2}\psi\left(2^j. - k\right)$ and $\tilde{\psi}_{(j,k)}$ is the dual of $\psi_{(j,k)}$. Since the set $\left\{\psi_{(j,k)}\right\}$ forms a wavelet frame, then its dual $\left\{\tilde{\psi}_{(j,k)}\right\}$ forms a dual wavelet frame. Each basis function in $\left\{\psi_{(j,k)}\right\}$ satisfies the dilation equation, that is [20–22]:

$$\psi(t) = \sqrt{2}\sum_{k\in\mathbb{Z}} g[k]\psi(2t - k). \tag{3.19}$$

where $g[k]$ is a half band digital low pass FIR filter associated with the scaling function, from which the set $\left\{\psi_{(j,k)}\right\}$ is generated. Moreover, each basis function in $\left\{\tilde{\psi}_{(j,k)}\right\}$ satisfies the dilation equation as:

$$\tilde{\psi}(t) = \sqrt{2}\sum_{k\in\mathbb{Z}} \tilde{g}[k]\tilde{\psi}(2t+k). \tag{3.20}$$

where $\tilde{g}[k]$ is the dual of $g[k]$.

Wavelet frames and their dual frames can be established by an exact reconstruction two-channel filter bank. Such a two-channel filter bank is composed from an analysis stage $(g[k], h[k])$ and a synthesis stage $(\tilde{g}[k], \tilde{h}[k])$, and these filters satisfy the following conditions [17–22]:

$$\delta[l] = \sum_{k\in\mathbb{Z}} g[k]\tilde{g}[2l-k], \text{ for } l \in \mathbb{Z}. \tag{3.21}$$

$$\sqrt{2} = \sum_{k\in\mathbb{Z}} g[k] = \sum_{k} \tilde{g}[k]. \tag{3.22}$$

$$g[k] = -(-1)^k \tilde{h}[k-1]. \tag{3.23}$$

$$h[k] = (-1)^k \tilde{g}[k-1]. \tag{3.24}$$

where $\delta[l]$ is the dirac delta. The bi-orthogonal scaling functions have been used in [20], [22], and [23] to generate phaselet basis functions. In these works, the use of bi-orthogonal scaling functions has been based on the fact that bi-orthogonal scaling functions can generate basis functions with high symmetry. Such basis function have the advantage of producing a FIR filter with linear phase responses[19].

The realization of a phaselet frame, by stages of two-channel filter banks, can be accomplished by selecting half-band FIR filters $g_p, h_p, \tilde{g}_p$, and $\tilde{h}_p$, which are associated with a set of phaselet basis functions $\{\alpha_m\}_{m=0}^{M-1}$. For a signal $x \in L^2(\mathbb{R})$, it can be

processed by phaselet frames (realized by stages of two-channel filter banks) as:

$$x = \frac{1}{M} \sum_{m=0}^{M-1} \left(\sum_{k \in \mathbb{Z}} \left(x * (g_p)_m \right) * (\tilde{g}_p)_m + \sum_{k \in \mathbb{Z}} \left(x * (h_p)_m \right) * \left(\tilde{h}_p \right)_m \right). \tag{3.25}$$

where $*$ is the convolution operation. In this work, the bi-orthogonal 1.3 scaling function is selected to generate phaselet basis functions, which are used to provide FIR filters. These FIR filters are used to construct the desired two-channel filter bank in order to implement the phaselet frames. The scaling function of the *bior1.3* and its magnitude spectrum are shown in Figure 3.1.

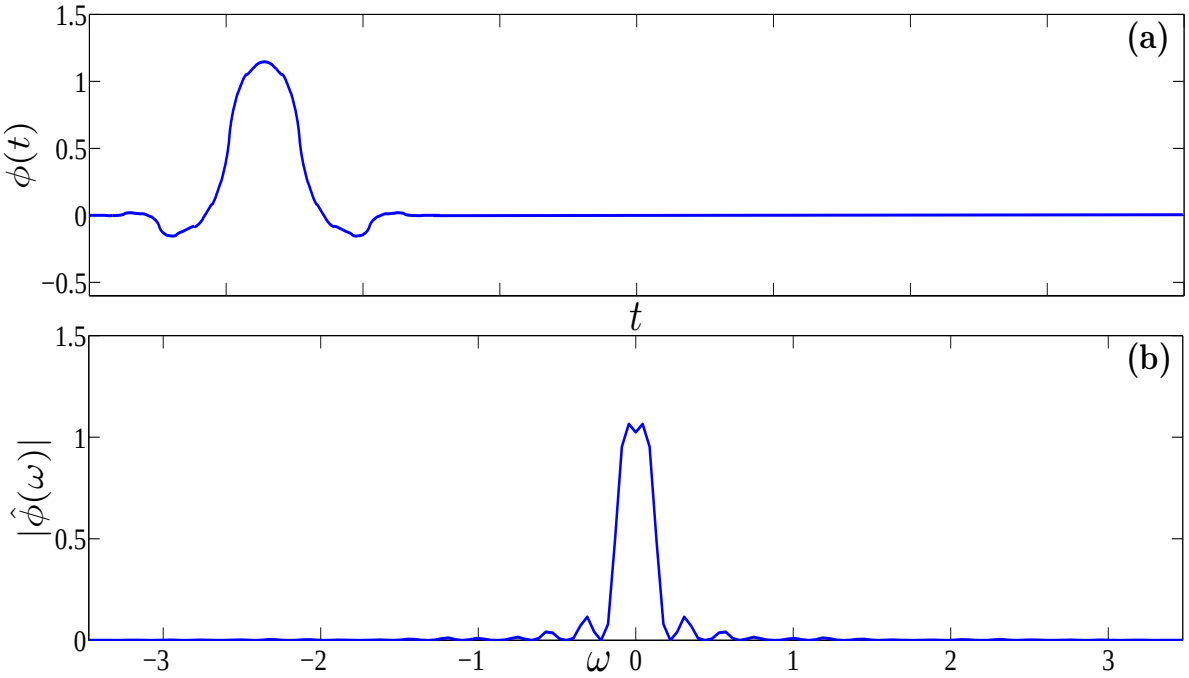

Figure 3.1: The scaling function of the *bior1.3*: (a) the scaling function $\phi(t)$ and (b) the magnitude spectrum $|\hat{\phi}(\omega)|$

It is to be noted that the selection of bi-orthogonal 1.3 scaling function is made as a trade-off between computational requirements and the density of generated basis functions [22]. The generation of the phaselet basis functions can be achieved by employing equation (3.16), where the set of phases $\{\tau_m\}_{m=0}^{M-1}$ is selected for $M = 6$

as:

$$\{\tau_m\} = \left\{0,\ -\frac{2\pi}{6},\ -\frac{4\pi}{6},\ -\frac{6\pi}{6},\ -\frac{8\pi}{6},\ -\frac{10\pi}{6}\right\}. \tag{3.26}$$

The setting of $M = 6$ is made to reduce the computational burden, as the 6 phaselet frames will process the apparent power $|\bar{S}|$ during each iteration. Since these 6 phaselet frames are produced by a bi-orthogonal scaling function, their high symmetry can facilitate an acceptable resolution of the calculated phase of $|\bar{S}|$ at each iteration. The selection of $\{\tau_m\}$ produces 6 phaselet basis functions, that can be substituted in equations (3.19) and (3.20) in order to obtain coefficients for the FIR filters. A MATLAB code is developed to solve the dilation equations for each phaselet basis function in order to obtain the coefficients of the low pass and high pass FIR filters g_p and h_p. The magnitude and phase responses of g_p and h_p are shown in Figure 3.2 and Figure 3.3.

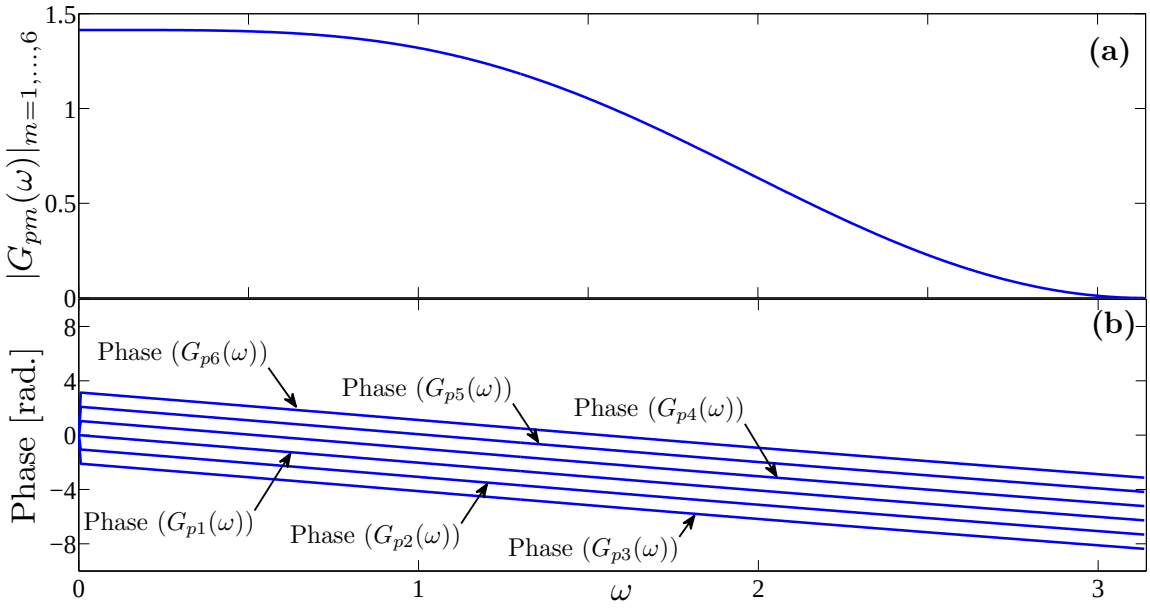

Figure 3.2: The low pass FIR filters associated with generated phaselet basis functions: (a) the magnitude spectrum of each $G_{pm}(\omega),\ m = 1, \ldots, 6$ and (b) the phase for each $G_{pm}(\omega)$.

Figure 3.2 shows that the 6 low pass FIR filters associated with the generated phase-

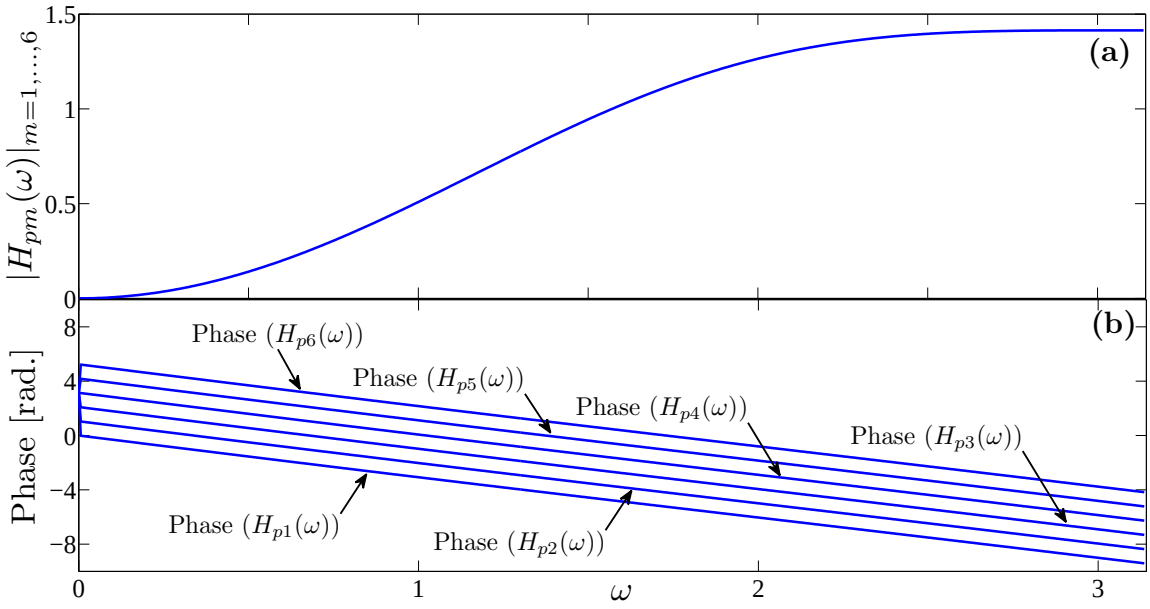

Figure 3.3: The high pass FIR filters associated with generated phaselet basis functions: (a) the magnitude spectrum of each $H_{pm}(\omega),\ m = 1, \ldots, 6$ and (b) the phase for each $H_{pm}(\omega)$.

let basis functions (using the bi-orthogonal scaling function 1.3) have an identical magnitude spectra, while each one of these FIR filters has its own linear phase shift. A similar notice can be made for the 6 high pass FIR filters, where Figure 3.3 shows that these high pass FIR filters have the same magnitude spectra, and each filter has its own linear phase. The structure of these 6 FIR filters can ensure that processing any signal will be more oriented towards extracting the phase of each frequency component present in the processed signal.

3.5 Summary

This chapter overviewed the phaselet analysis and its possible employment for estimating the phase of the processed signal. As the processed signal is filtered by low and high pass FIR filters, the outputs of these filters can be viewed as orthogonal

components of the processed signal. Since the used FIR filters have linear phase responses, the phase of the processed signal can be obtained from the outputs of the FIR filters. This feature of phaselet frames allows processing the iterated $|\bar{S}|$ in order to calculate its phase θ. The next chapter provides the realization of the Newton iteration(to estimate $|\bar{S}|$), when combined with the 6 phaselet frames constructed in this chapter.

Chapter 4

Performance of Newton-Phaselet Method

4.1 General

The focus of this work is on residential and small commercial loads (RSCLs), which have their power consumption measured by single phase (1ϕ) power meters. Chapter 2 and Chapter 3 have provided the foundation for modeling residential and small commercial (RSCL) loads using the ZIP model approach. as Chapter 2 has presented the ZIP model for any load, where the active and reactive power demands by a load are required. However, such requirements can not be met in RSCL, as the active power consumption is measured by a power meter. In order to overcome this challenge, Chapter 3 presented a numerical approach based on combining Newton's iteration (to calculate $|\bar{S}|$) and phaselet frames (to calculate θ). The Newton Phaselet method can provide values for θ using values of measured P, and thus meeting the requirement of the ZIP model. This Chapter develops an algorithm for implementing the Newton-phaselet method. In addition, this chapter presents and discusses the

performance of the Newton-phaselet method for several sets of collected power meter readings from different residential units in Fredericton, New Brunswick, Canada. It should be noted that the collected data was obtained by using power meters that are designed based on the IEEE 1459 Standard (see Appendix A), and provide only values for the active power (energy consumption as power consumed over time). The developed Newton-phaselet approach takes the read power signal and calculates $|\bar{S}|$, θ, Q and P_c in order to complete the ZIP model and retrieve the load status using K_{pF}.

4.2 Developing an Algorithm for the Newton Phaselet Method

In general, the active power P can be related to the reactive power Q through the power factor (PF) as:

$$Q = P\tan(\theta);\ \theta = \cos^{-1}(PF). \tag{4.1}$$

Equation (4.1) indicates that the angle θ is required to determine a value for Q using a value of P. Such a limitation of 1ϕ power meters can be overcome by employing numerical methods, in particular, Newton iterations. In order to employ Newton iterations to determine PF or θ, the following system of non-linear equations is set for the iterations as:

$$0 = Q - P\tan(\theta). \tag{4.2}$$

$$\Delta\theta = \frac{\Delta Q - \tan(\theta)\Delta P}{P + P\tan^2(\theta)}. \tag{4.3}$$

One can see from equation (4.3) that $\Delta\theta$ is a function in $\tan(\theta)$, which has infinite values for $\theta = \pm\pi/2$. This property of $\tan(\theta)$ may complicate converging to the desired solution. Alternatively, the apparent power $\bar{S}$ can be a simpler approach, to calculate θ, than the reactive power approach. The apparent power $\bar{S}$ can be related to P as:

$$P = |\bar{S}|\cos(\theta). \tag{4.4}$$

$$\Delta P = \cos(\theta)\Delta|\bar{S}| - |\bar{S}|\sin(\theta)\Delta\theta. \tag{4.5}$$

Equations (4.4) and (4.5) can provide a setting for Newton iterations, where θ can be determined using the 6 phaselet frames as discussed in Chapter 3. As the value of $|\bar{S}|$ is iterated, the 6 phaselet frames will be used to process the iterated values $|\bar{S}|$ in order to determine a value of θ at each iteration. In this setting, values of $|\bar{S}|$ during the iterations will be stored in an array $\boldsymbol{A}$, that is:

$$\boldsymbol{A} = \left[|\bar{S}|^{(0)}\ |\bar{S}|^{(1)}\ \ldots\ |\bar{S}|^{(n)}\right]. \tag{4.6}$$

where $|\bar{S}|^{(n)}$ is the value of $|\bar{S}|$ at iteration n. The array $\boldsymbol{A}$ will be decomposed using the 6 phaselet frames during each iteration, in order to produce a direct component (s_d) and a quadrature (s_q) component. These components are defined as:

$$s_d = \boldsymbol{A} * LPF_1 + \boldsymbol{A} * LPF_2 + \boldsymbol{A} * LPF_3 + \boldsymbol{A} * LPF_4 + \boldsymbol{A} * LPF_5 + \boldsymbol{A} * LPF_6. \tag{4.7}$$

$$s_q = \boldsymbol{A} * HPF_1 + \boldsymbol{A} * HPF_2 + \boldsymbol{A} * HPF_3 + \boldsymbol{A} * HPF_4 + \boldsymbol{A} * HPF_5 + \boldsymbol{A} * HPF_6. \tag{4.8}$$

A value of θ at iteration n can be determined using s_d and s_q as:

$$\theta^{(n)} = \tan^{-1}\left(\frac{s_q}{s_d}\right). \tag{4.9}$$

Determining θ can be interpreted as the total contributions of projecting $|\bar{S}|$ on the 6 phaselet frames as iterations converge to a solution (i.e. $(\delta P)^{(n)} \longrightarrow 0$). As θ is obtained using the phaselet frames (4.9), the Newton iterations can be realized to provide a value for $|\bar{S}|$. During iterations calculated values of θ and $|\bar{S}|$ can provide a calculated value for active power $Pc^{(n)}$ as:

$$Pc^{(n)} = |\bar{S}|^{(n)} \cos(\theta^{(n)}) \tag{4.10}$$

The mismatch in the active power at iteration n can be obtained as:

$$\delta P^{(n)} = P - Pc^{(n)} \tag{4.11}$$

The determination of $\delta P^{(n)}$ allows stating the change in $|\bar{S}|$ as:

$$\delta S^{(n)} = \frac{\delta P^{(n)}}{\cos(\theta^{(n)})} + \delta\theta^{(n)}|\bar{S}|^{(n)} \tan(\theta^{(n)}) \tag{4.12}$$

$$|\bar{S}|^{(n+1)} = |\bar{S}|^{(n)} + \delta S^{(n)} \tag{4.13}$$

where:

$$\delta\theta^{(n)} = \theta^{(n)} - \theta^{(n-1)} \tag{4.14}$$

$$\delta PF^{(n)} = -\delta\theta^{(n)} \sin(\theta^{(n)}) \tag{4.15}$$

Using the equations for ΔPs and ΔPz

$$\Delta P_S = -\frac{P\Delta\theta \tan(\theta)}{1 - \Delta\theta \tan(\theta) + \tan^2(\theta)} \tag{4.16}$$

$$\Delta P_Z = -\frac{V^2}{Z}\Delta\theta \sin(\theta) \tag{4.17}$$

Equations (4.16) and (4.17) are combined with equation (4.12) to provide a formulation for K_{pF}, that is:

$$K_{pf}[n] = \frac{\Delta P[n] - P\Delta P_Z[n] - 2P\Delta P_S[n]}{P\Delta P_Z[n] + 2P\Delta P_S[n]}. \tag{4.18}$$

$$K_{qf}[n] = \frac{\Delta Q[n] - P\Delta Q_Z[n] - 2P\Delta Q_S[n]}{P\Delta Q_Z[n] + 2P\Delta Q_S[n]}. \tag{4.19}$$

The analysis presented in equations (4.6) through (4.19) indicates that the newton-phaselet method requires performing four sets of calculations for each value of P. These calculations are:

1) Calculating $|\bar{S}|$: These calculations are performed by using the Newton iterations. At each iteration one element of vector $\boldsymbol{A}$ is determined

2) Calculating θ: These calculations are performed by using the phaselet frames to process the vector $\boldsymbol{A}$ at each iteration. The phaselet frames are realized by the HPF FIR filters

3) Calculating Q: These calculations are performed after $|\bar{S}|$ and θ are determined a value for Q for a given value of P can be calculated as: $Q = P\tan(\theta)$.

4) Calculating K_{pf} and K_{qf}: These calculations are performed after θ is determined. A value of K_{pF} is determined using equation (4.18) and K_{qf} is determined using equation (4.19)

The aforementioned calculations can be made into an algorithm, which is shown in the flowchart of Figure 4.1.

The determination of K_{pF} can be used to identify the appliances that are ON or OFF. The identification of the status of appliance, using K_{pF} is accomplished based

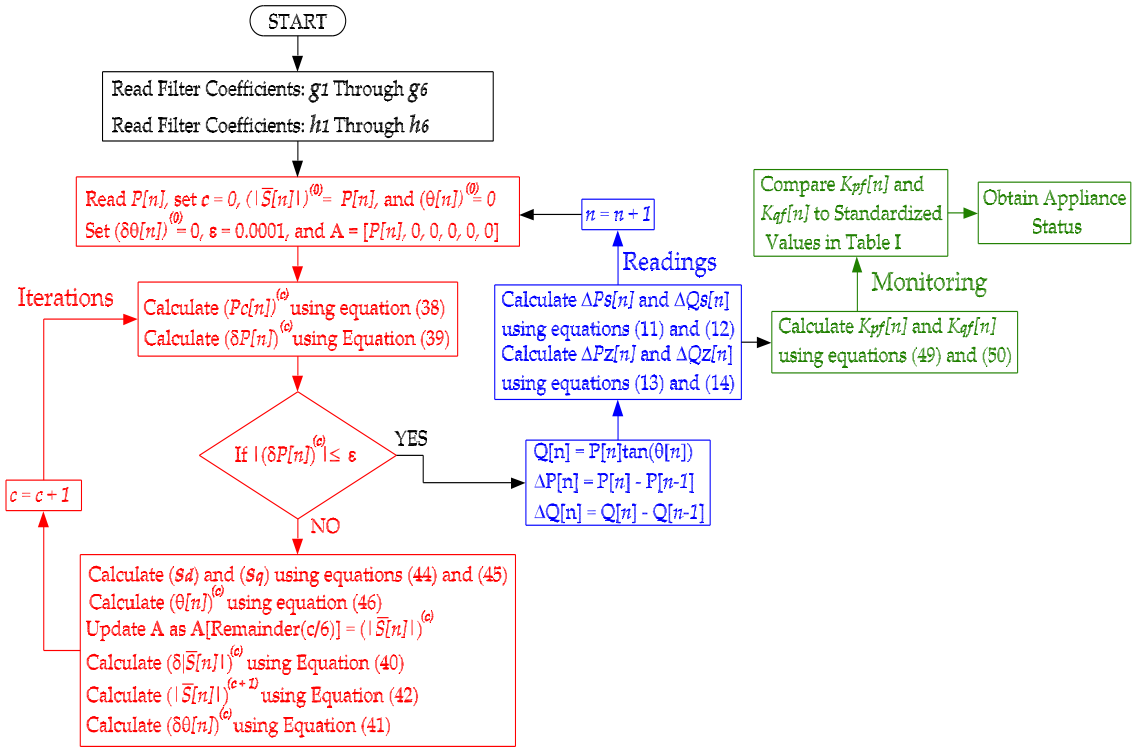

Figure 4.1: Flowchart for ZIP modeling using phaselet frames. Table 4.1 provides values of K_{pF} and K_{qF} for different household appliances.

on a standardised value, of K_{pF} for different appliances. These values of K_{pF} are provided in Table 4.1

4.3 Performance Results

The algorithm in Figure 4.1 was realized by a MATLAB/SIMULINK model for performance evaluation. The developed model had its inputs as values of P (measured), while its outputs were ON-OFF status of appliances. In this thesis, status of sample appliances are shown to demonstrate the performance of the Newton-phaselet method. The sample appliances are:

a) Water heater;

Table 4.1: Standardized values for K_{pF} and K_{qF}

Appliance	K_{pF}	K_{qF}
1ϕ AC	0.90	-2.70
Water Heater	2.40	0.05
Range top oven	2.40	0.02
Baseboard Heater	2.40	0.07
Clothes washer	3.00	1.80
Refrigerator	0.53	-1.50
Fluorescent lights	1.00	-2.80
Motorised tools	2.50	1.20
Fan Motors	2.90	1.70

b) Stove;

c) Fridge;

d) Heater.

The tests of the Newton-phaselet method were carried out using several sets of collected data from different residential units in Fredericton, New Brunswick, Canada. The test data was collected over different seasons of 2013, 2014 and 2015. It should be noted that the algorithm can provide the status of other appliances. However, the previous appliances are widely considered as target appliances for demand response programs. The following subsections present and discuss results obtained for test data. It should be noted that the tolerance ϵ (in the flowchart of Figure 4.1) was set to $\epsilon = 0.0001$. The value of ϵ was selected to ensure a finite number of Newton iterations for each value of P (measured), which was the input for the algorithm. Finally, in all results plotted in this section, the values of Pc (calculated by the developed algorithm) were scaled by 0.75 in order to distinguish Pc from P

4.3.1 First Data Set

This set of data was measured using PowerHouse Dynamics emonitor digital metering system [31], which can provide measured values for 130 energy consumptions on various appliances in a residential unit. The first data set was recorded between 8:06 AM until 11:00 AM during a day in March 2013. This set of data was collected over the 3 hour interval at a rate of 1 sample/5 minutes. The calculated values of $|\bar{S}|$, θ and Q, along with the values of P (inputs to the algorithm) for the first data set are shown in Figure 4.2. The values of θ (calculated) and P (measured) were used to complete the ZIP model in order to evaluate K_{pF}. The evaluation of K_{pF} allowed for identification of the ON-OFF status of the water heater, fridge, stove and heater in the residential unit, for which P was measured. Figure 4.3 shows the ON-OFF status for the aforementioned appliances. The results in Figure 4.2 show that the Newton-phaselet method was able to converge with good accuracy. This convergence could be seen from the close match between Pc and P (measured) shown in Figure 4.2 (a). 4.2 (b) shows the calculated $|\bar{S}|$, where the convergence of Pc implied accurate values of $|\bar{S}|$. Similar observations can be made for the calculate values of θ (in Figure 4.2 (c)) and Q (in Figure 4.2 (d)).

The accurate calculation of Q allowed determining K_{pF} (using the ZIP model), which was used together with Table 4.1 to identify the ON-OFF status of the water heater, fridge, stove, and heater as shown in Figure 4.3. The accuracy of identifying the status of the target appliances was demonstrated by comparing the output of the Newton-phaselet method with the measured power consumption for the water heater and fridge, as shown in Figure 4.4. The identified ON-OFF status of the water heater and fridge demonstrated good agreement with the measured power consumptions of these two appliances. For purposes of demonstrating the accuracy

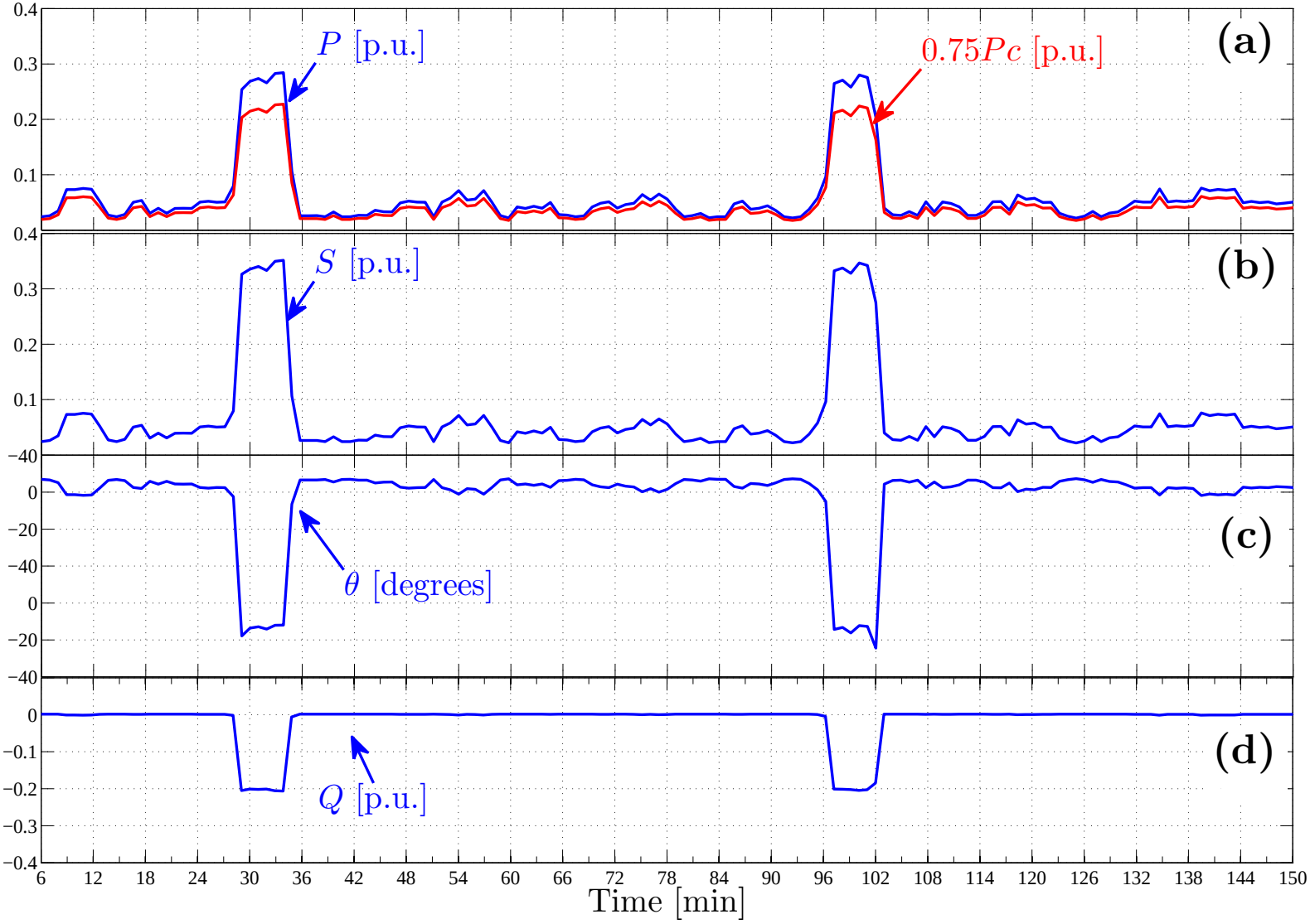

Figure 4.2: Performance results from the first data set: (a) measured power and calculated power in per unit, (b) calculated apparent power $|\bar{S}|$ in per unit, (c) calculated angle θ in degrees, and (d) calculated reactive power Q in per unit.

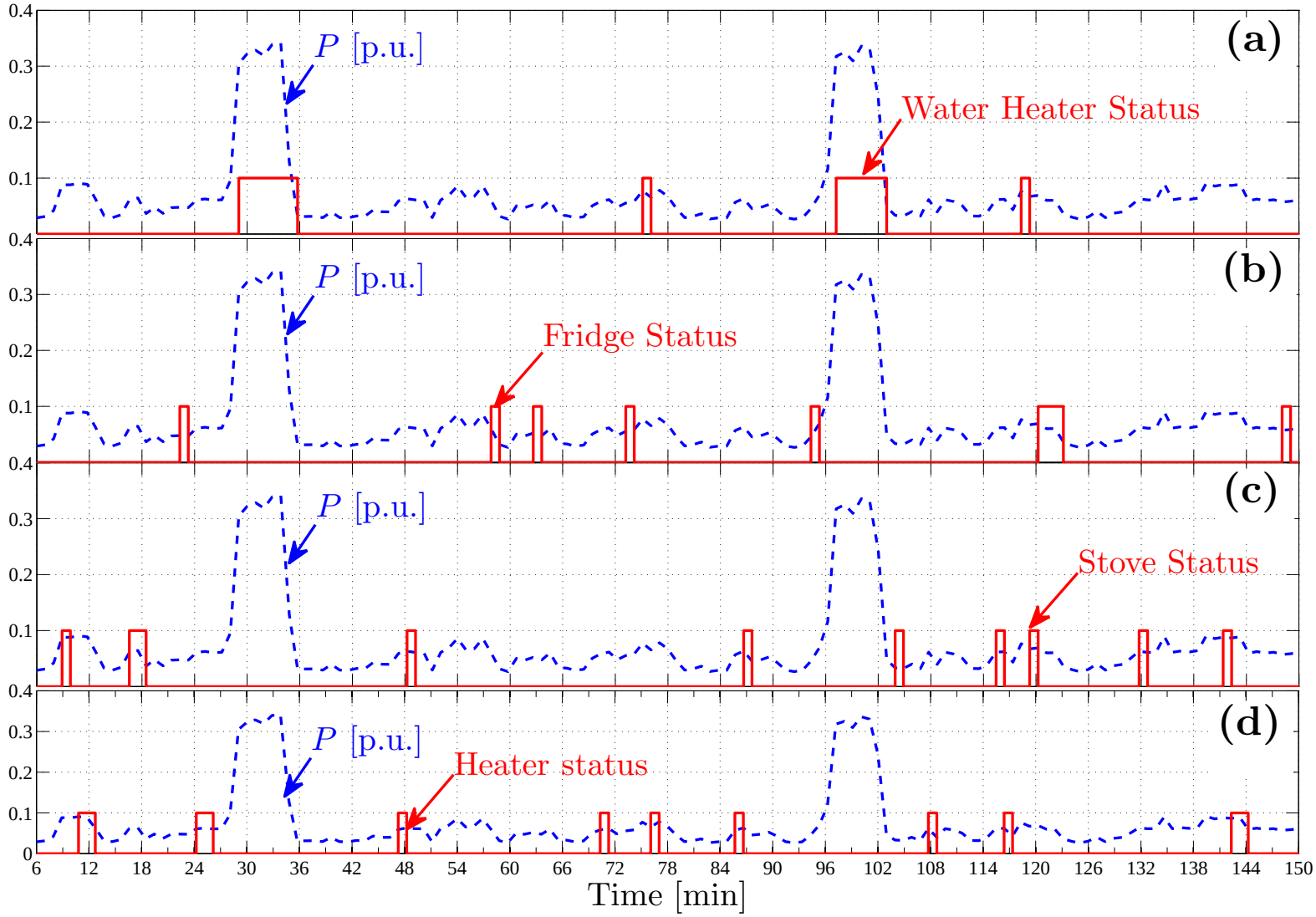

Figure 4.3: Performance results from the first data set: (a) water heater ON-OFF status, (b) fridge ON-OFF status, (c) stove ON-OFF status, and (d) heater ON-OFF status.

of the newton-phaselet, the actual and determined ON-OFF status for the water heater and fridge, along with K_{pF} are shown in Figure 4.3.

4.3.2 Second Data Set

This second data set was retrieved over a time interval of 24 hours in Fredericton, New Brunswick during the month of October 2014. This set of data was collected using an Itron CENTRON® II. The second set of data was collected over the 24 hour interval at a rate of 1 sample/1 minute. Figure 4.5 shows the calculated values of $|\bar{S}|$, θ and Q, as well as P for the second data set. The values of the calculated θ and measured P were used to complete the ZIP model, which provided values for K_{pF}. Obtained values of K_{pF} allowed the identification of the ON-OFF status of the water heater, fridge, stove and heater in the residential unit, where P was measured. The results in Figure 4.5 show consistent ability of the Newton-phaselet method to converge with proper accuracy. This convergence could be seen in Figure 4.5 (a) which indicated a close match between Pc and P. Furthermore, Figure 4.5 (b) shows the calculated $|\bar{S}|$, where the convergence of Pc indicated accurate values of $|\bar{S}|$. In a similar manner, the convergence of Pc supported the accurate calculation of both θ (in Figure 4.5 (c)) and Q (in Figure 4.5 (d)). The accurate calculation of Q allowed determining K_{pF} (using the ZIP model), which was employed, along with Table 4.1 to identify the ON-OFF status of the water heater, fridge, stove, and heater. The ON-OFF status of these appliances are shown in Figure 4.6.

4.3.3 Third Data Set

The third data set was retrieved over a time interval of 24 hours in Fredericton, New Brunswick during the month of January 2015. This set of data was collected using

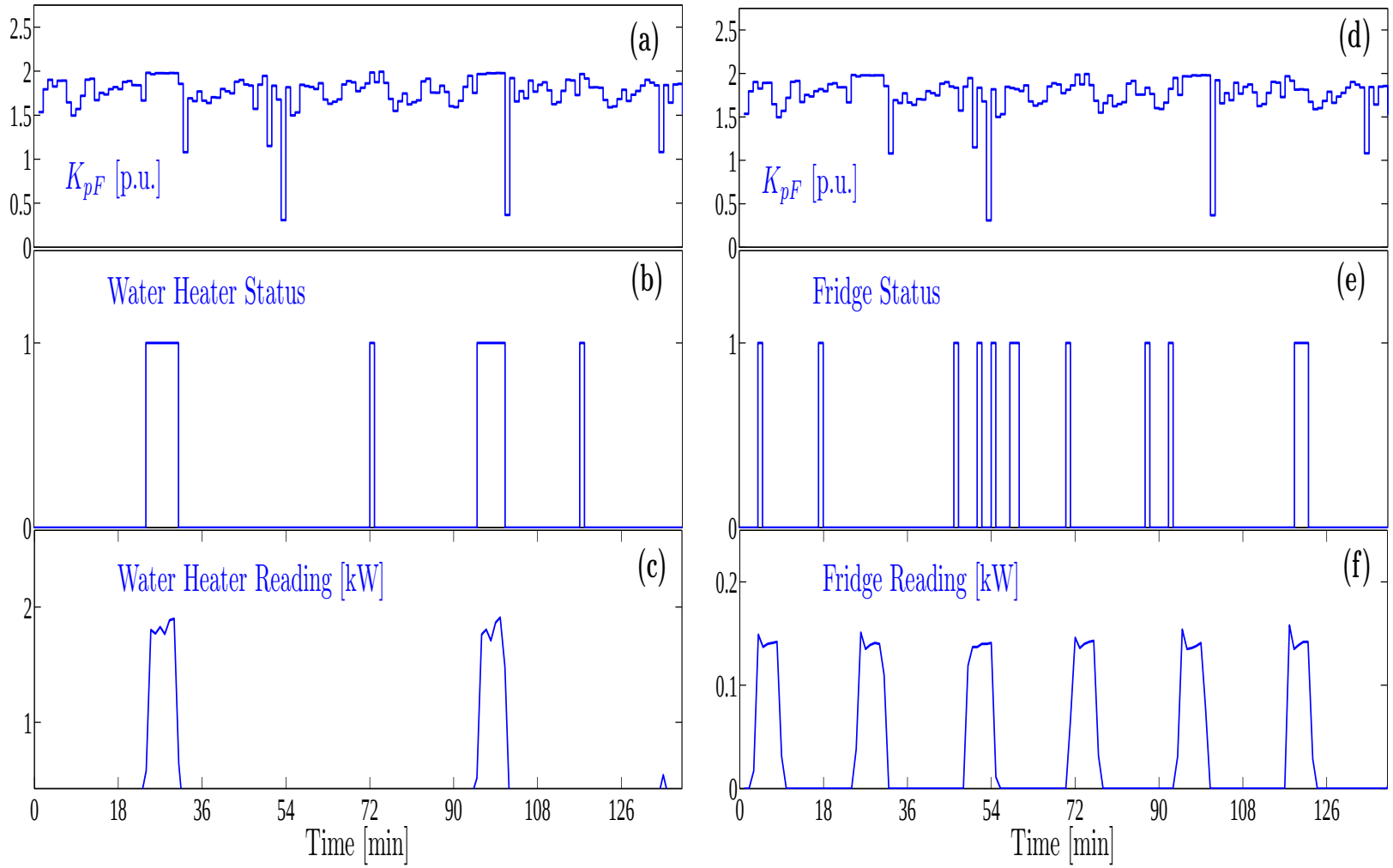

Figure 4.4: Performance results from the first data set: (a) K_{pF}, (b) water heater ON-OFF status, (c) actual water heater readings, (d) K_{pF}, (e) fridge ON-OFF status, and (f) actual fridge readings.

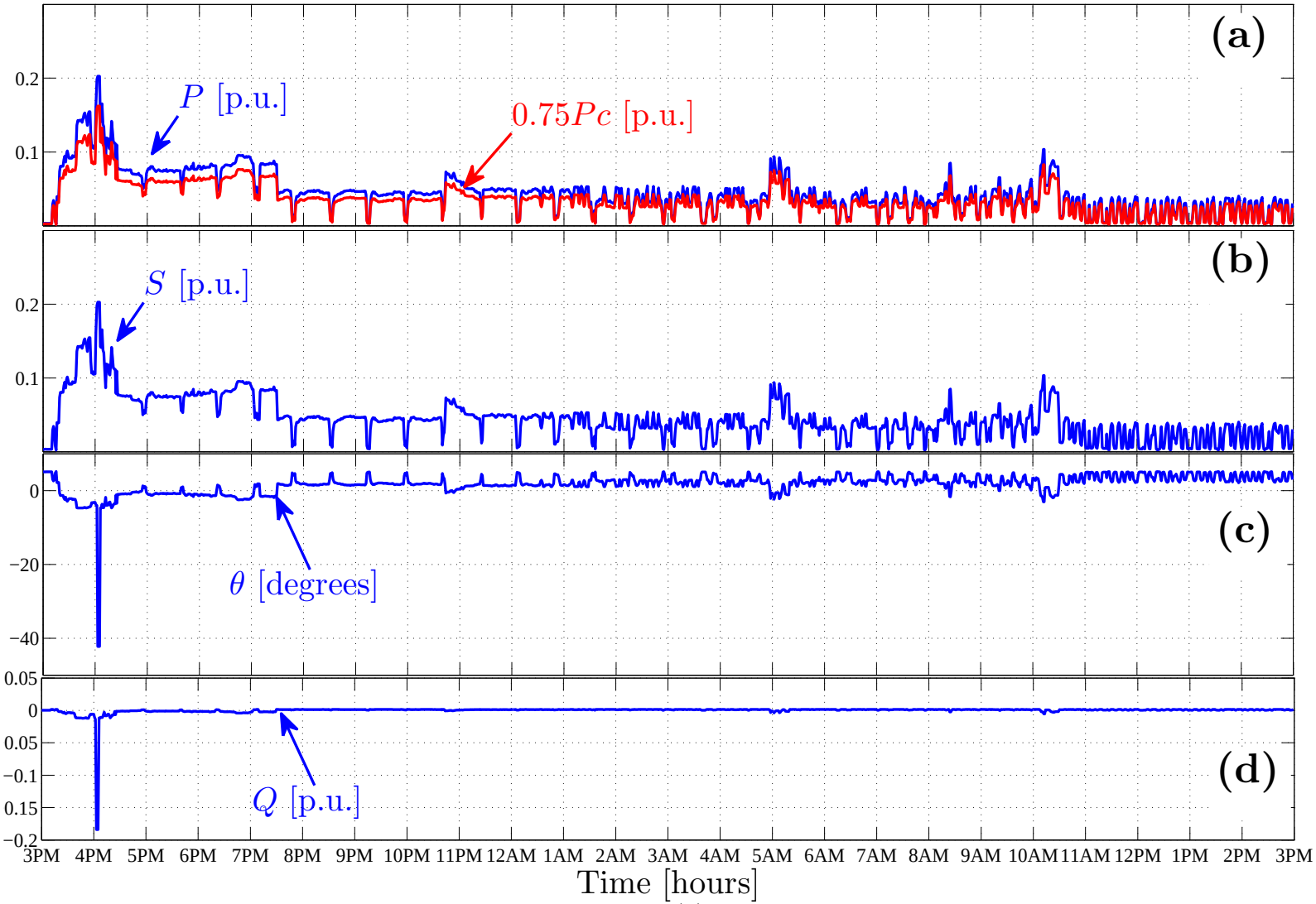

Figure 4.5: Performance results from the second data set: (a) measured power and calculated power in per unit, (b) calculated apparent power $|\bar{S}|$ in per unit, (c) calculated angle θ in degrees, and (d) calculated reactive power Q in per unit.

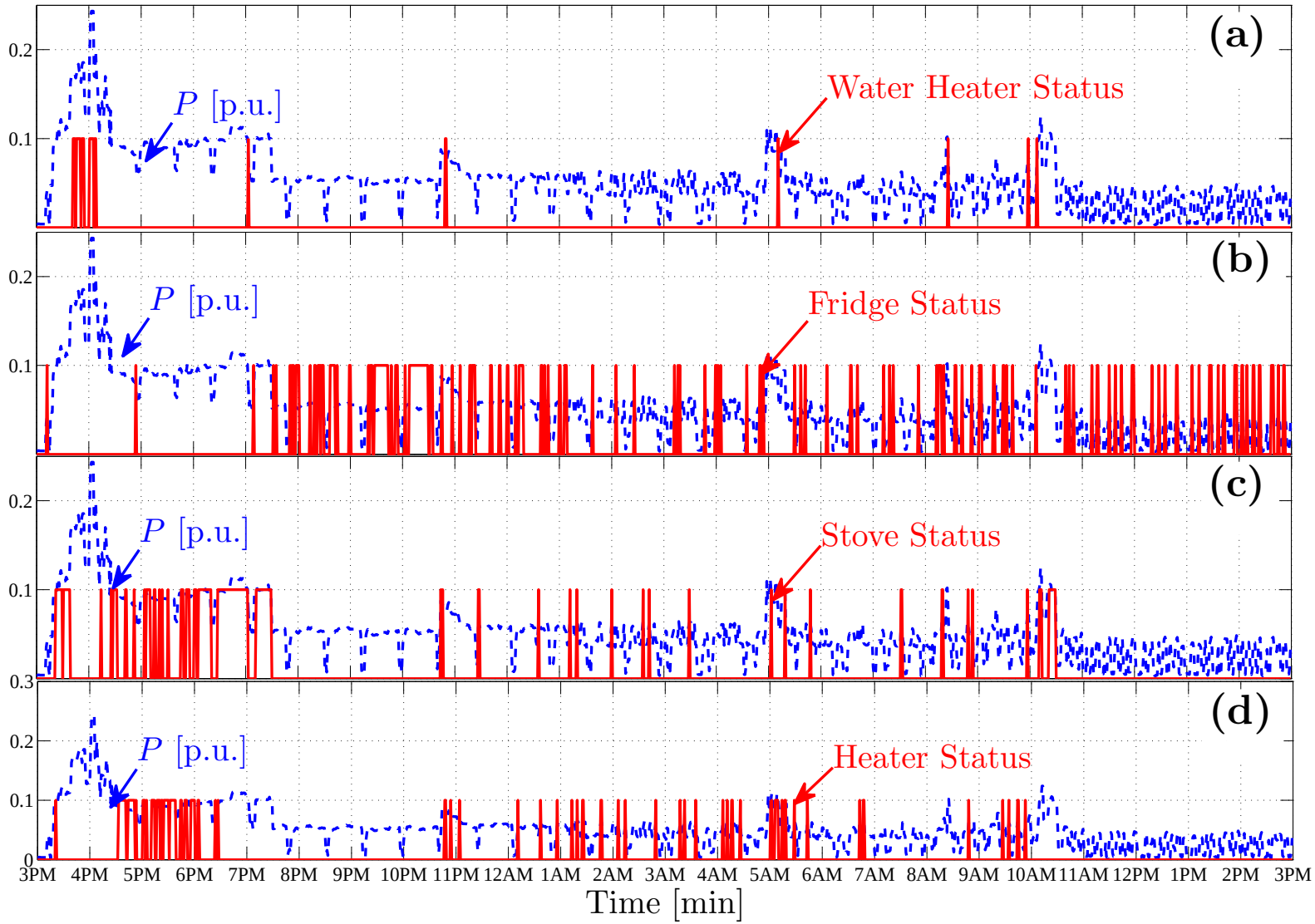

Figure 4.6: Performance results from the second data set: (a) water heater ON-OFF status, (b) fridge ON-OFF status, (c) stove ON-OFF status, and (d) heater ON-OFF status.

an Itron CENTRON® II, at a rate of 1 sample/1 minute. Figure 4.7 for the third data set shows the calculated values of $|\bar{S}|$, θ, Q, and P. The ZIP model which was completed using the calculated θ and measured P, was used to calculate K_{pF}. The obtainedK_{pF} allows for identification of the ON-OFF status of the water heater, fridge, stove and heater in the household for which P was measured. Figure 4.7 shows that the Newton-phaselet method was able to converge accurately which was due to the close match between Pc and measured P which can be seen in Figure 4.7 (a). Figure 4.7 (b) shows the calculated $|\bar{S}|$, where the convergence of Pc implied accurate values of $|\bar{S}|$. Similar observations can be made for the calculate values of θ (in Figure 4.7 (c)) and Q (in Figure 4.7 (d)). The accurate calculation of Q allowed determining K_{pF} (using the ZIP model), which was used together with Table 4.1 to identify the ON-OFF status of the water heater, fridge, stove, and heater as shown in Figure 4.8.

Table 4.2 summarizes the accuracy in identifying the appliances (water heater, stove, fridge and heater) considered as target appliances in the previous tests. It should be noted that the identification accuracy was determined as the difference between the status obtained through the algorithm and the actual status of each target appliance.

Table 4.2: Performance criteria for individual loads

Criteria for	Identification Accuracy
Water Heater	86%
Fridge	57%
Stove	83%
Heater	80%

In order to provide further insight, Table 4.3 provides the execution time and memory requirement for the Newton-phaselet algorithm for each tested data.

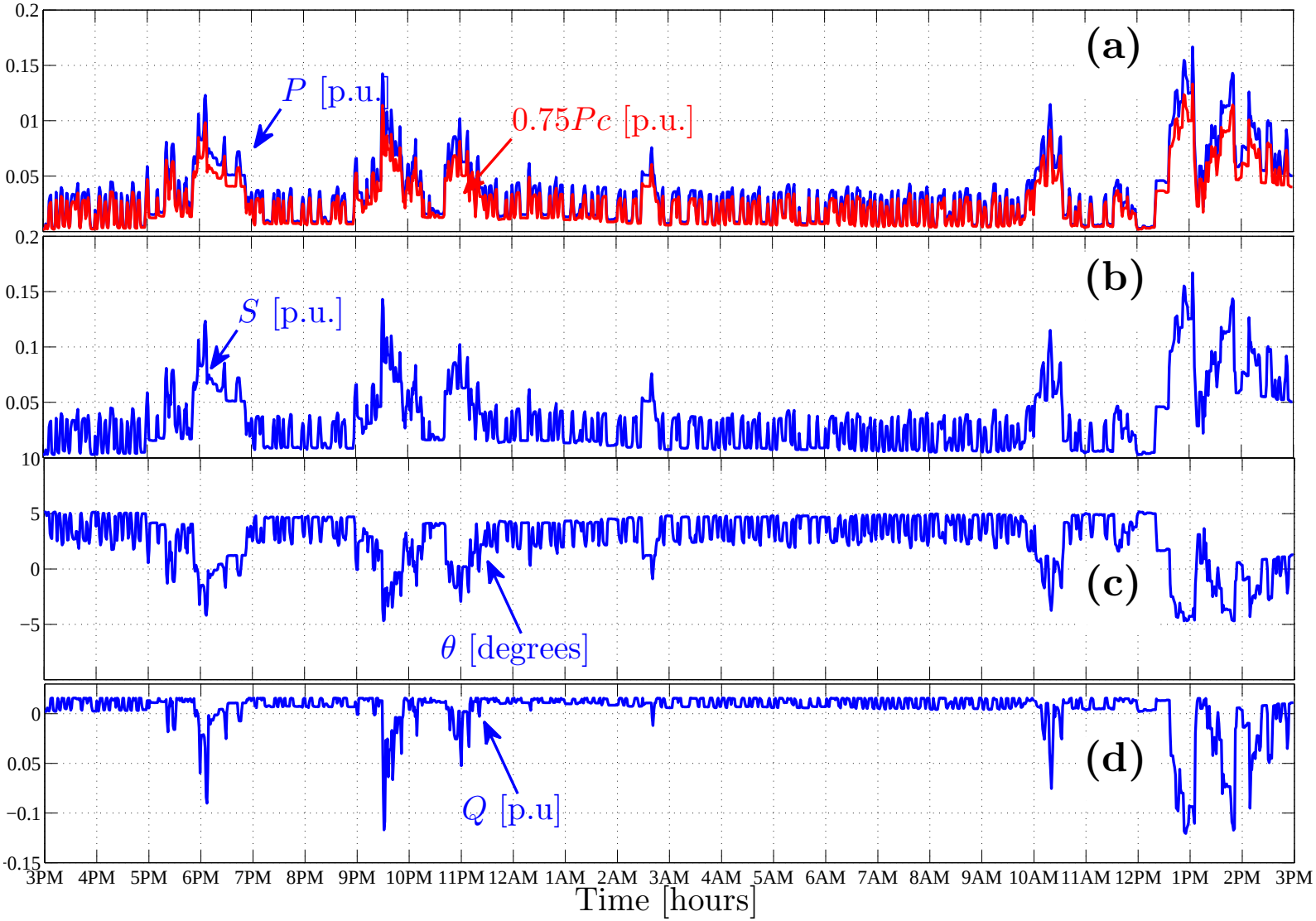

Figure 4.7: Performance results from the third data set: (a) measured power and calculated power in per unit, (b) calculated apparent power $|\bar{S}|$ in per unit, (c) calculated angle θ in degrees, and (d) calculated reactive power Q in per unit.

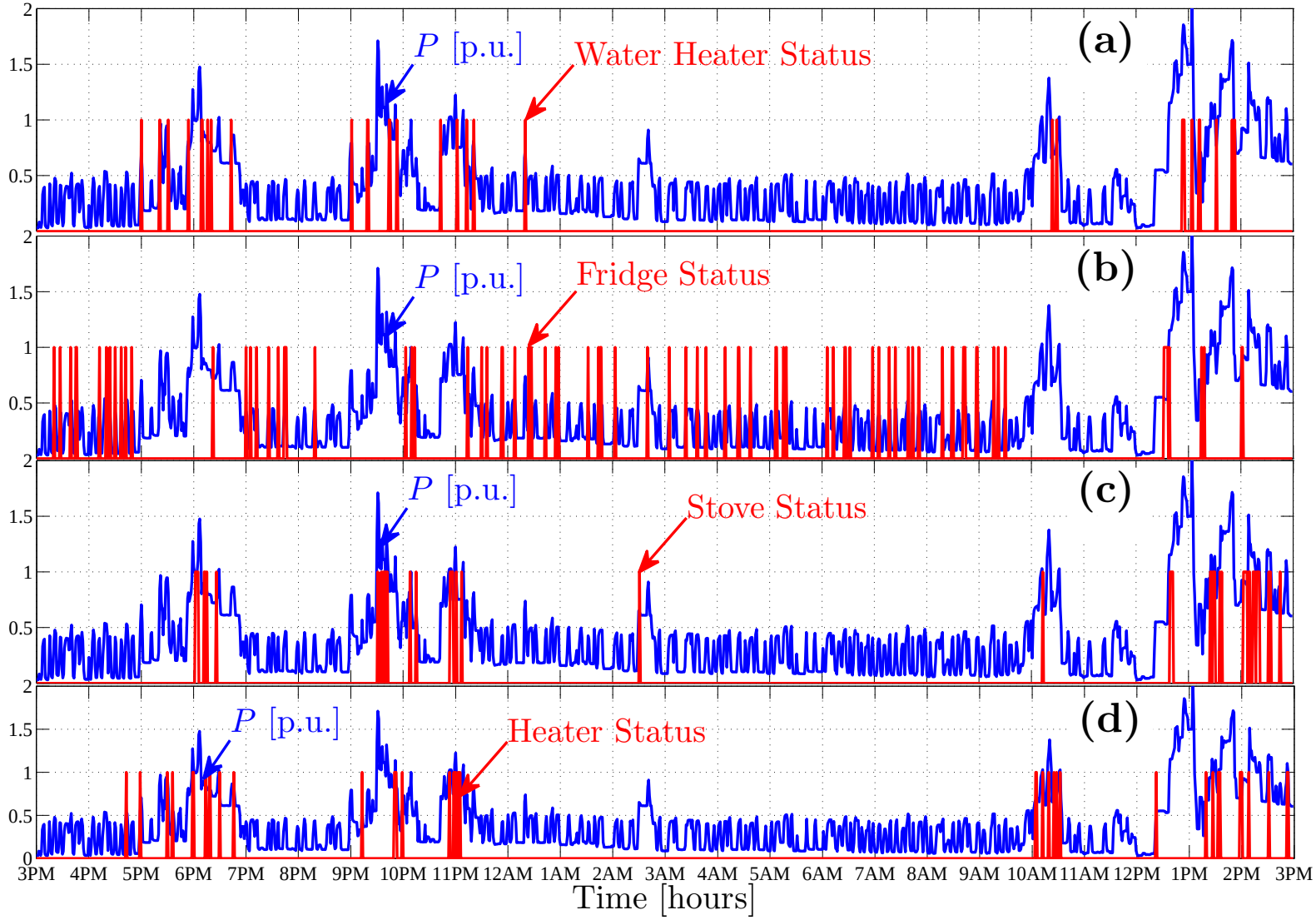

Figure 4.8: Performance results from the second data set: (a) water heater ON-OFF status, (b) fridge ON-OFF status, (c) stove ON-OFF status, and (d) heater ON-OFF status.

Table 4.3: Performance criteria of all data sets

Criteria	First Data Set	Second Data Set	Third Data Set
Time of Execution	10 μsec.	10 μsec.	10 μsec.
Memory Requirement	100 kB	100 kB	100 kB

For the sake of highlighting the advantages of the developed method, a comparison with the artificial neural network (ANN) and Markov chain (MC) based methods is provided in terms of the memory requirements, computational requirement, training data, accuracy, and the need for historical data. The summary of this comparison is listed in Table 4.4.

Table 4.4: Performance comparison of the Newton phaselet, ANN, and MC methods:

Criteria	Newton phaselet	ANN	MC
Memory requirement	Low	High	High
Computational requirement	Low	High	High
Training data	Not Required	Required	Required
Accuracy	77%	80%	87.5%
Historical Data	Not Required	Required	Not Required

The performance of the ANN and MC based methods were obtained from the details in references [1, 11, 13].

The data in Table 4.3 demonstrates simple implementation of the Newton-phaselet algorithm as indicated by the execution time and memory requirements. In addition, the performance comparison summarized in Table 4.4 indicates the advantages that can be offered by the Newton phaselet method over the ANN and MC based methods. Finally, the data in Table 4.2, Table 4.3 and Table 4.4, along with test results provide support to the application of the Newton-phaselet method in smart grid functions.

4.4 Summary

This chapter has presented the development of an algorithm for the Newton-phaselet method. The developed algorithm has been implemented using MATLAB/SIMULINK software for purposes of evaluating its performance. Three sets of data have been used in the performance evaluation. These sets of data have been provided as collections of measured power of three different residential units in Fredericton, New Brunswick during 2013, 2014 and 2015. In all performance tests, the algorithm has shown a good ability to converge, along with good consistency in the accuracy of the obtained results. The results obtained from these tests have demonstrated that the Newton-phaselet method is insensitive to load types and rate of data sampling. Finally, performance results confirmed the ability of the developed method to provide accurate ON-OFF status of target appliances without the need for training.

Chapter 5

Conclusions and Future Work

5.1 Summary

The interests in implementing smart grid functions have motivated several research works that aim to optimize the modeling and control of the target loads within any utility power system. One of the widely used smart grid functions is the demand response, that is applied to residential and small commercial loads. Similar to the other smart grid functions, the research activities in optimizing the demand response have been mostly focused on developing models for the target residential and small commercial loads. Desired models are mainly required to accurately provide the ON-OFF status of controllable appliances in target residential or small commercial loads. Available models are based on statistical and pattern recognition approaches, which mandate collecting significant amounts of data for training and tuning.

This thesis has presented an alternative approach based on the ZIP model, where the needs for training and tuning data can be eliminated. However, the ZIP model requires values for the active power P and the reactive power Q of the load in order to decompose the power consumptions among appliances. As typical power meters

only provide P, the determination of Q becomes a challenge. Such a challenge can be overcome by employing numerical methods and concepts of signal processing. The combination of Newton iterations and phaselet frames has been implemented as an algorithm to provide Q, which allows for utilizing the ZIP model in residential and small commercial loads.

Performance results of the Newton-phaselet method have demonstrated good accuracy, along with insensitivity to the sampling rate of the measured power. In addition, performance results have shown that accurate updates of ON-OFF statuses of appliances can be achieved by the proposed method without needs for training data. The simplicity and accuracy of the Newton-phaselet method supports its validity and applicability in demand response programs.

5.2 Conclusions

The research work in this thesis has been focused on developing a new approach for modeling RSCLs and determining the ON-OFF status for the appliances in these loads. The motivation for this work has been driven by the growing interests in simplifying the implementation of a smart grid function, in particular, the demand response. The method developed and tested in this thesis has been based on combining Newton iterations and phaselet frames in order to calculate a value of reactive power Q. The calculated Q and measured active power P can complete the ZIP model, which has standardized parameters for the power consumption of each appliance. These standardized parameters can provide the ON-OFF status of appliances. The Newton-phaselet algorithm has been developed and successfully tested for different sets of collected power meter data. The features of the developed algorithm together with its performance allow drawing the following conclusions:

- The ZIP model approach can offer simpler and more optimal realization of demand response than statistical and pattern recognition approaches.
- Phaselet frames can provide effective and accurate tool for processing the active power in order to calculate the magnitude and phase of the apparent power ($|\bar{S}|$ and θ).
- The combination of Newton iterations and phaselet frames neither affects the stability of phaselet-frames nor does it affect the convergence of Newton iterations.
- The ZIP model can provide accurate determination of ON-OFF status of appliances without needs for collecting data for training and tuning.
- The Newton-phaselet algorithm can offer an optimized structure for non-intrusive load modeling (NILM) for smart grid applications.

5.3 Contributions

The research work presented in this thesis has made several contributions that can be summarized as:

- The employment of the ZIP model for obtaining ON-OFF status of appliances in RSCLs.
- The development of a modeling approach for realizing NILM without needs of training or tuning.
- The successful realization of phaselet frames, using FIR filters, for processing signals in power system applications (e.g. determining $|\bar{S}|$, θ, and Q using only P).

- The development of a functional algorithm to determine the ON-OFF status of appliances using only power meter readings, which is done on a one-reading basis.

- The successful evaluation of the performance of the Newton-phaselet method in completing the ZIP model in order to determine the ON-OFF status of appliances in RSCLs.

5.4 Future Work

The developed Newton-phaselet approach for determining the ON-OFF status of appliances in RSCLs can provide grounds for future research works in different areas, some of such research works can be identified as:

- Introducing new features for identifying the ON-OFF status for appliances that do not have standardized values of K_{pF}(e.g. Television, dryers, microwaves, etc.). One possible feature can be expressed by the changes of $|\bar{S}|$ with respect to changes in θ

- Utilizing the phaselet frames for designing new phase-locked-loop (PLL) devices for possible applications in grid-connected power electronic converters and renewable energy systems.

- Extending the developed Newton-phaselet algorithm for applications in industrial loads.

- Adapting the ZIP model for applications in micro-grid systems, where load modeling is critical for maintaining stable functions of the micro-grid systems.

Bibliography

[1] M. Dong, P. C. M. Meira, W. Xu, and W. Freitas, "An Event Window Based Load Monitoring Technique for Smart Meters," *IEEE Trans. on Smart Grid*, Vol. 3, No. 2, pp. 787–796, 2012.

[2] J. D. Hobby, A.r Shoshitaishvili, and G. H. Tucci, "Analysis and Methodology to Segregate Residential Electricity Consumption in Different Taxonomies," *IEEE Trans. on Smart Grid*, Vol. 3, No. 1, pp. 217–224, 2012.

[3] D. H. O. McQueen, P. R. Hyland, and S. J. Watson, "Monte Carlo Simulation of Residential Electricity Demand for Forecasting Maximum Demand on Distribution Networks," *IEEE Trans. on Power Systems*, Vol. 19, No. 3, pp. 1685–1689, 2004.

[4] D. Schatsky and C. Wheelock, "Home Energy Management," *[Online], Available: http://www.pikeresearch.com/research/*, 2011.

[5] S. M. Amin and B. F.Wollenberg, "Toward a Smart Grid," *IEEE Power Energy Magazine*, Vol. 3, No. 5, pp. 34–41, September/October 2005.

[6] *The smart grid: An introduction,* U.S. Department of Energy, 2011, *[Online], Available: http://www.oe.energy.gov/SmartGridIntroduction.html*, 2011.

[7] A. M. García, M. Kessler, J. A. Fuentes, and E. G. Lázaro, "Probabilistic Characterization of Thermostatically Controlled Loads to Model the Impact of Demand Response Programs," *IEEE Trans. on Power Systems*, Vol. 26, No. 1, pp. 241–251, 2011.

[8] S. W. Heunis and R. Herman, "A Probabilistic Model for Residential Consumer Loads," *IEEE Trans. on Power Systems*, Vol. 17, No. 3, pp. 621–625, 2002.

[9] A. Capasso, W. Grattieri, R. Lamedica, and A. Prudenzi, "A Bottom-Up Approach to Residential Load Modeling," *IEEE Trans. on Power Systems*, Vol. 9, No. 2, pp. 957–964, 1994.

[10] J. Kondoh, N. Lu, and D. J. Hammerstrom, "An Evaluation of the Water Heater Load Potential for Providing Regulation Service," *IEEE Trans. on Power Systems*, Vol. 26, No. 3, pp. 1309–1316, 2011.

[11] J. W. Taylor and A. Siddharth, "Short-Term forecasting of Anomalous Load Using Rule-Based Triple Seasonal Methods" *IEEE Trans. on Power Systems*, August 2013.

[12] A. Khotanzadf, E. Zhou and H. Elragel, "A Neuro-Fuzzy Approach to Short-Term Load Forecasting in A Price Sensitive Environment", *IEEE Trans. on Power Systems*, November 2002.

[13] A. G. Baklrtzls, V. Petrldls, S. J. Klartzls, and M. C. Alexladls, , "A Neural Network Term Load Forecasting Model For The Greek Power System", *IEEE Trans. on Power Systems*, May 1996.

[14] D. E. Wahl, P. H. Eichel, D. C. Ghiglia and C. V. Jakowatz jr., *Phase Gradient Autofocus-A Robust Tool for High Resolution SAR Phase Correction*, *IEEE trans. on Aerospace and Electronic Systems*, July 1994.

[15] F. Cruz-Roldan, P. Martin-Martin and J. Saez-Landete*A Fast Windowing-Based Technique Exploiting Spline Functions for Designing Modulated Filter Banks*, *IEEE Trans. on Circuits and Systems*, January 2009.

[16] J. Liang, S. Ng, G. Kendall, and J. Cheng, Load Signature Study-Part II: Disaggregation Framework, Simulation, and Applications, IEEE Trans. On Power Delivery, Vol. 25, No. 2, pp. 561-569, 2010.

[17] R. A. Gopinath, "Phaselets of Framelets," *IEEE Trans. on Signal Processing*, Vol. 53, No. 5, pp. 1794–1806, 2005.

[18] R. Yu, "Theory of Dual-Tree Complex Wavelets," *IEEE Trans. on Signal Processing*, Vol. 56, No. 9, pp. 4263–4273, 2008.

[19] R. A. Gopinath, "The Phaselet Transform–An Integral Redundancy Nearly Shift-Invariant Wavelet Transform," *IEEE Trans. on Signal Processing*, Vol. 51, No. 7, pp. 1792–1805, 2003.

[20] I. W. Selesnick, "The Design of Approximate Hilbert Transform Pairs of Wavelet Bases," *IEEE Trans. on Signal Processing*, Vol. 50, No. 5, pp. 11441152, 2002.

[21] J. Kovačcević and A. Chebira, "Life Beyond Bases: The Advent of Frames (Part I)," *IEEE Signal Process. Mag.*, Vol. 24, No. 4, pp. 86104, July, 2007.

[22] J. Kovačcević and A. Chebira, "Life Beyond Bases: The Advent of Frames (Part II)," *IEEE Signal Process. Mag.*, Vol. 24, No. 5, pp. 115125, September, 2007.

[23] *Definitions for the Measurement of Electric Quantities Under Sinusoidal, Non-sinusoidal, Balanced, or Unbalanced Conditions, IEEE Std. 1459*, 2010.

[24] A. Cataliotti, V. Cosentino, and S. Nuccio, "Comparison of Nonactive Powers for the Detection of Dominant Harmonic Sources in Power Systems," *IEEE Trans. on Instrumentation and Measurement*, Vol. 57, No. 8, pp. 1554–1561, 2008.

[25] V. V. Terzija, V. Stanojević, M. Popov, and L. V. der Sluis, "Digital Metering of Power Components According to IEEE Standard 1459-2000 Using the Newton-Type Algorithm," *IEEE Trans. on Instrumentation and Measurement*, Vol. 56, No. 6, pp. 2717–2724, 2007.

[26] S. Lee, B. Kwon, and S. Lee, "Joint Energy Management System of Electric Supply and Demand in Houses and Buildings," *IEEE Trans. on Power Systems*, Vol. 29, No. 6, pp. 2804–2812, 2014

[27] S. M. M. Agah and H. A. Abyaneh, "Effect of Load Models on Probabilistic Characterization of Aggregated Load Patterns," *IEEE Trans. on Power Systems*, Vol. 26, No. 2, pp. 811–819, 2011.

[28] S.A. Pourmousavi and M.H. Nehrir, "Introducing Dynamic Demand Response in the LFC Model," *IEEE Trans. on Power Systems*, Vol. 29, No. 4, pp. 1562–1572, 2014.

[29] S. Son, S. H. Lee, D. H. Choi, K. B. Song, J. D. Park, Y. H. Kwon, K. Hur, and J. W. Park, "Improvement of Composite Load Modeling Based on Parameter Sensitivity and Dependency Analyses," *IEEE Trans. on Power Systems*, Vol. 29, No. 1, pp. 242–250, 2014.

[30] Y. Wi, S. Joo, and K. Song , "Holiday Load Forecasting Using Fuzzy Polynomial Regression With Weather Feature Selection and Adjustment,", *IEEE Trans. on Power Systems*, Vol. 27, No. 2, pp. 596–603, 2012.

[31] *eMonitor Hardware Guide, Rev. 1.0,* Powerhouse Dynamics, Newton, Massachusetts, USA, 2012.

Appendix A

Definitions of Power Components in IEEE 1459-2000 Standard

For a 1ϕ system, the IEEE 1459-2000 Standard provides definitions for all components of power under any voltage and current. These definitions include sinusoidal and non-sinusoidal voltages and/or currents that can be defined as [23–25]:

$$v = \sqrt{2}V_1 \sin(\Omega_s t - \theta_1) + \sqrt{2}\sum_{m\neq 1} V_m \sin(m\Omega_s t - \theta_m) \tag{A.1}$$

$$i = \sqrt{2}I_1 \sin(\Omega_s t - \gamma_1) + \sqrt{2}\sum_{m\neq 1} I_m \sin(m\Omega_s t - \gamma_m) \tag{A.2}$$

where $m \in \mathbb{Z}$ is the harmonic order. In addition, the rms values of the voltage and currents can be expressed as:

$$V_{\text{rms}} = \sqrt{V_1^2 + \sum_{m\neq 1} V_m^2} = \sqrt{V_1^2 + V_h^2} \tag{A.3}$$

$$I_{\text{rms}} = \sqrt{I_1^2 + \sum_{m\neq 1} I_m^2} = \sqrt{I_1^2 + I_h^2} \tag{A.4}$$

Equation (A.1), (A.2), (A.3), and (A.4) can be used to state the components of the power as [23–25]:

I- The active power P:

$$P = V_1 I_1 \cos(\theta_1 - \gamma_1) + \sum_{m \neq 1} V_m I_m \cos(\theta_m - \gamma_m) \tag{A.5}$$

II- The reactive power Q:

$$Q = V_1 I_1 \sin(\theta_1 - \gamma_1) + \sum_{m \neq 1} V_m I_m \sin(\theta_m - \gamma_m) \tag{A.6}$$

Appendix B

Tight Frames

If a set of basis functions, $\{\boldsymbol{\nu}_0, \boldsymbol{\nu}_1, \ldots, \boldsymbol{\nu}_p\}$ with $p \in \mathbb{Z}$ and $p < \infty$, spans a space $\mathcal{W}$, then any function λ can be projected onto $\mathcal{W}$. The projection of λ onto $\mathcal{W}$ provides an expansion of λ as [23–29]:

$$\lambda = \sum_p g_p \boldsymbol{\nu}_p; \quad g_p \in \mathbb{R}. \tag{B.1}$$

where the set of coefficients $\{g_p\}$ is obtained by the inner product operation as:

$$g_p = \langle \lambda, \nu_p \rangle \tag{B.2}$$

A subset of the basis functions, $\{\boldsymbol{\nu}_0, \boldsymbol{\nu}_0, \ldots, \boldsymbol{\nu}_d\}$ with $d \in \mathbb{Z}$ and $d < p$, are a frame in $\mathcal{W}$ if it satisfies the following condition:

$$A \left\|\lambda\right\|^2 \leq \sum_p |\left\langle \lambda, \boldsymbol{\nu}_p \right\rangle|^2 \leq B \left\|\lambda\right\|^2 ; \forall \lambda \in \mathcal{W}. \tag{B.3}$$

where $A \in \mathbb{R}$, such that $B \in \mathbb{R}$ and $0 < A \leq B < \infty$, are the lower and upper frame bounds, respectively. If $A = B$, then the frame is a tight frame.

Curriculum Vitae

Candidates full name:	Petrus Pijnenburg
Universities attended:	Bachelor in Electrical/Electronic Engineering
	Fontys University of Applied Sciences Eindhoven
	The Netherlands, Aug 2009 Jul 2013
	Major: Electrical/Electronic Engineering
	Minor: Mechatronics
Publications:	P. Pijnenburg, P. R. McGaw, and S. A. Saleh, " Phaselet Frame-Based Approach for Monitoring the Status of Appliances in Residential Loads," *To be submitted to IEEE Trans. on Power Systems*, April 2015.